Variations of Earth rotation from ring laser gyroscopes: one hundred years of rotation sensing with optical interferometry

U. Schreiber

Forschungseinrichtung Satellitengeodäsie,
Technische Universität München, Germany

Earth Rotation and Orientation are providing the link between the terrestrial (ITRF) and celestial reference frames (ICRF). Traditionally the Earth orientation parameters (EOPs) are observed by radio interferometry. The fixed positions of the quasars, along with measurement redundancy of a sufficiently large network, provide the long-term stability of the observations. For the short-term and the access to the instantaneous rotation axis of the Earth, VLBI is depending on suitable models, which still have some deficiencies. Optical interferometric rotation sensing with ring lasers in contrast provides direct access to the Earth rotation axis, a high resolution in the short-term, but are suffering from tiny non-reciprocal laser behavior causing drift in the long-term. Now, one hundred years after George Sagnac's important paper published in Comptes Rendus in 1913 the tools of modern quantum optics have matured to a point where they make ring lasers more than 12 orders of magnitude more sensitive than the early instrumentation in this field. The single component prototype ring laser G in Wettzell now resolves rotation rates of 10e-12 rad/s after one hour of integration and has demonstrated an impressive sensor stability over several month. The combination of VLBI and ring laser measurements offers an improved sensitivity for the EOPs in the short-term and the direct access to the Earth rotation axis. At the same time the progress in controlling the backscatter coupling in ring lasers has succeeded to reach the domain of 3 parts per billion for the relative uncertainty of the measured Earth rotation. This paper explores the prospects of optical Sagnac Interferometry in Geodesy at the Centennial of the Sagnac effect.

Earth: "The living Planet"

complex interaction
of coupled subsystems

large numbers of dynamic
processes over a wide range
of time scales

Resources of the Earth are
limited

Geodesy contributes to better
understanding by:

- mapping the figure and gravity field
- observing changes over time
- establishing reference frames

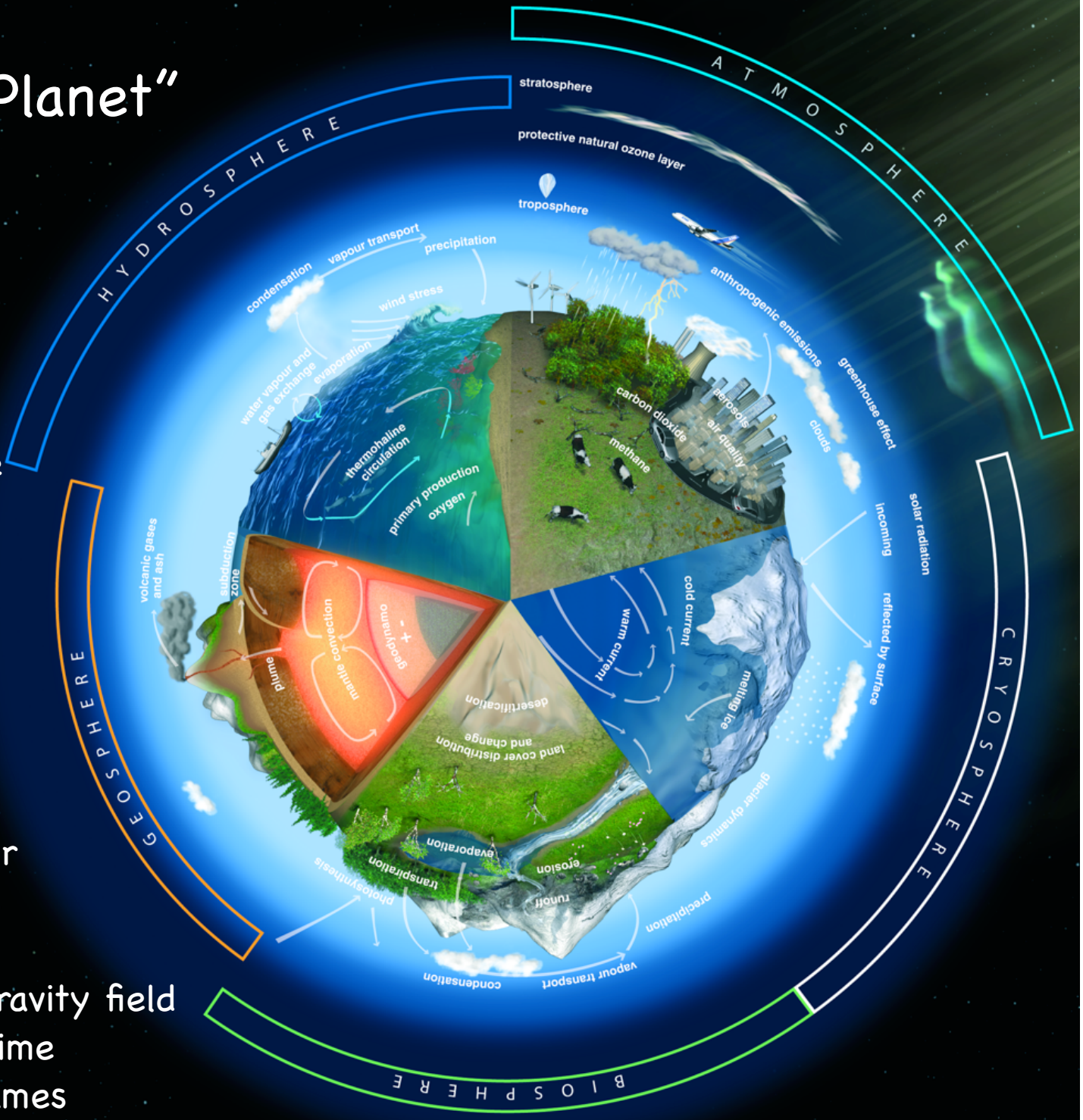

credits: ESA

Ocean. Mass Transport

ocean circulation
mass and heat transport
sea level height variation
Change of mass & volume

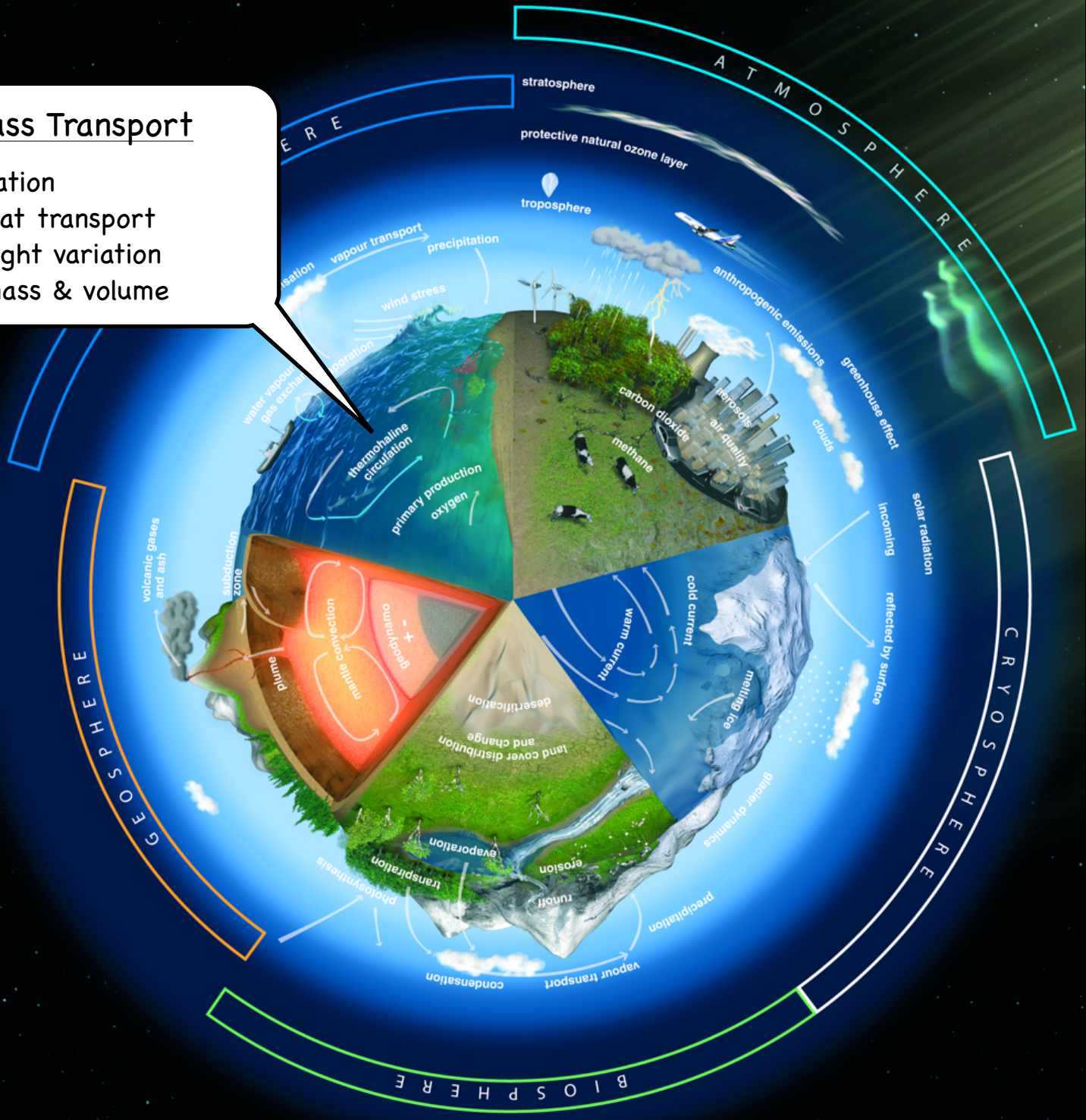

credits: ESA

Ocean. Mass Transport

ocean circulation
mass and heat transport
sea level height variation
Change of mass & volume

climate change

interaction of atmosphere & ocean
anthropogenic interaction

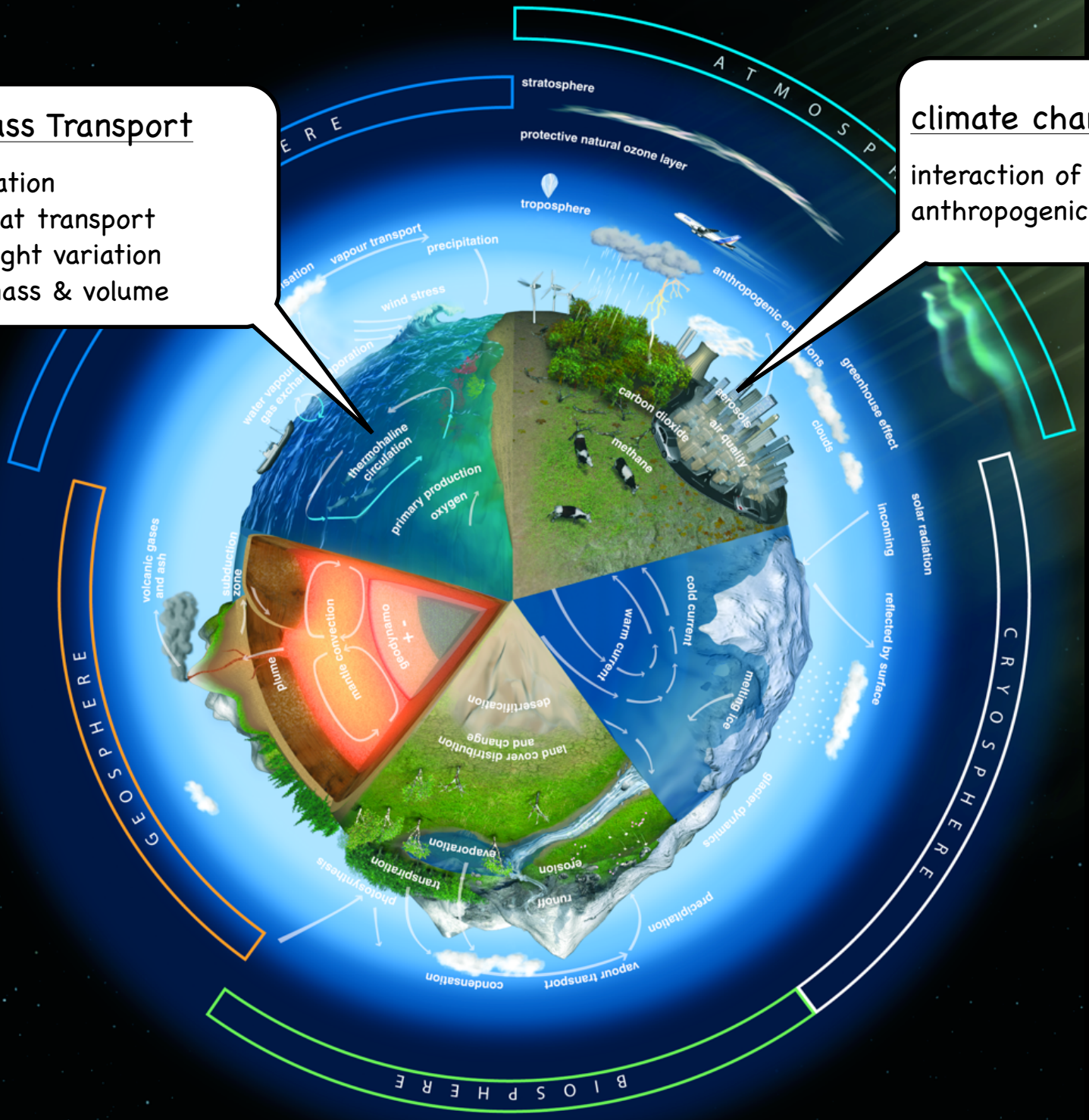

credits: ESA

Ocean. Mass Transport

ocean circulation
mass and heat transport
sea level height variation
Change of mass & volume

climate change

interaction of atmosphere & ocean
anthropogenic interaction

Icesheet variation

snow and ice coverage, dynamics
interaction with oceans

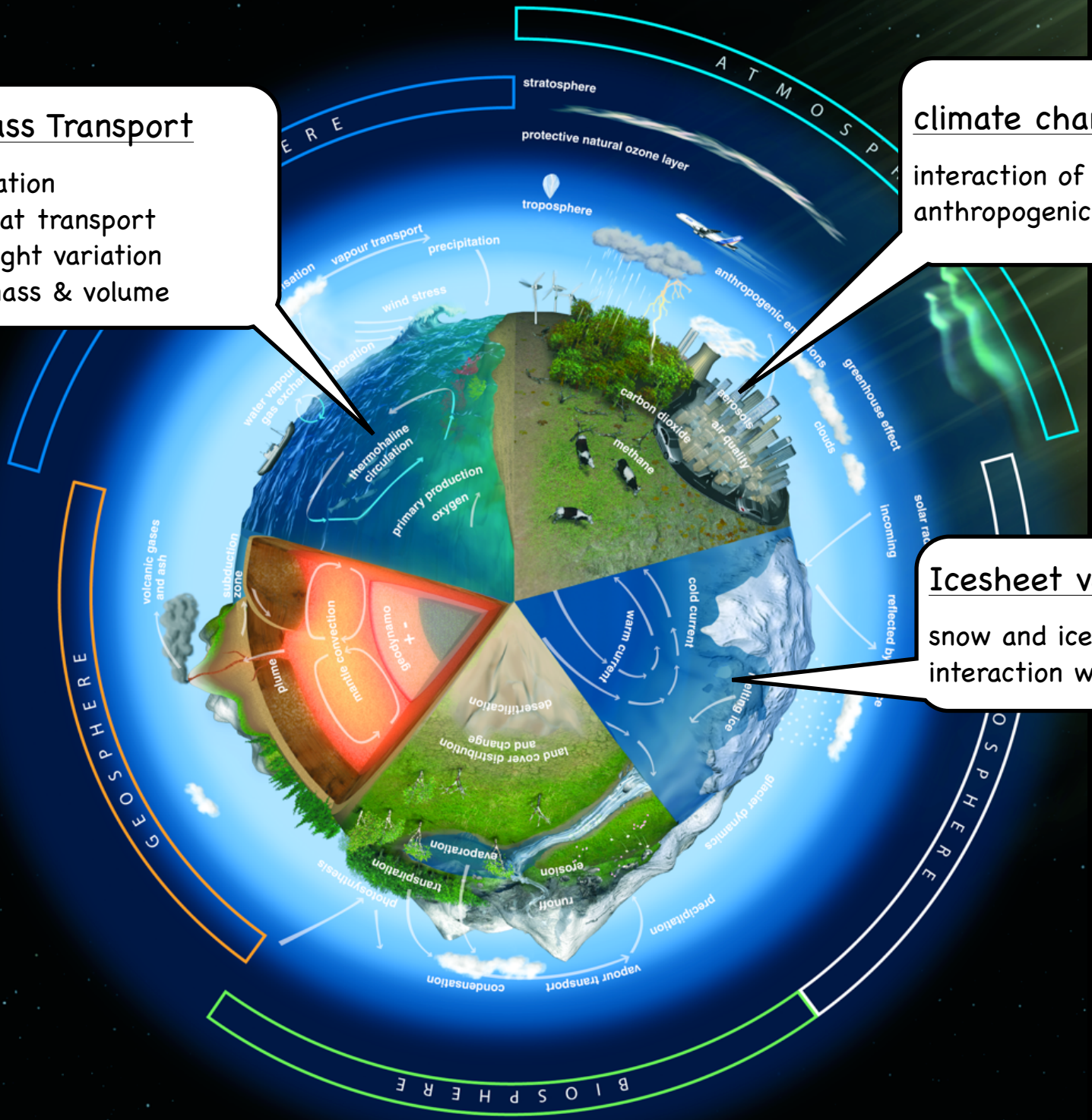

credits: ESA

Ocean. Mass Transport

ocean circulation
mass and heat transport
sea level height variation
Change of mass & volume

climate change

interaction of atmosphere & ocean
anthropogenic interaction

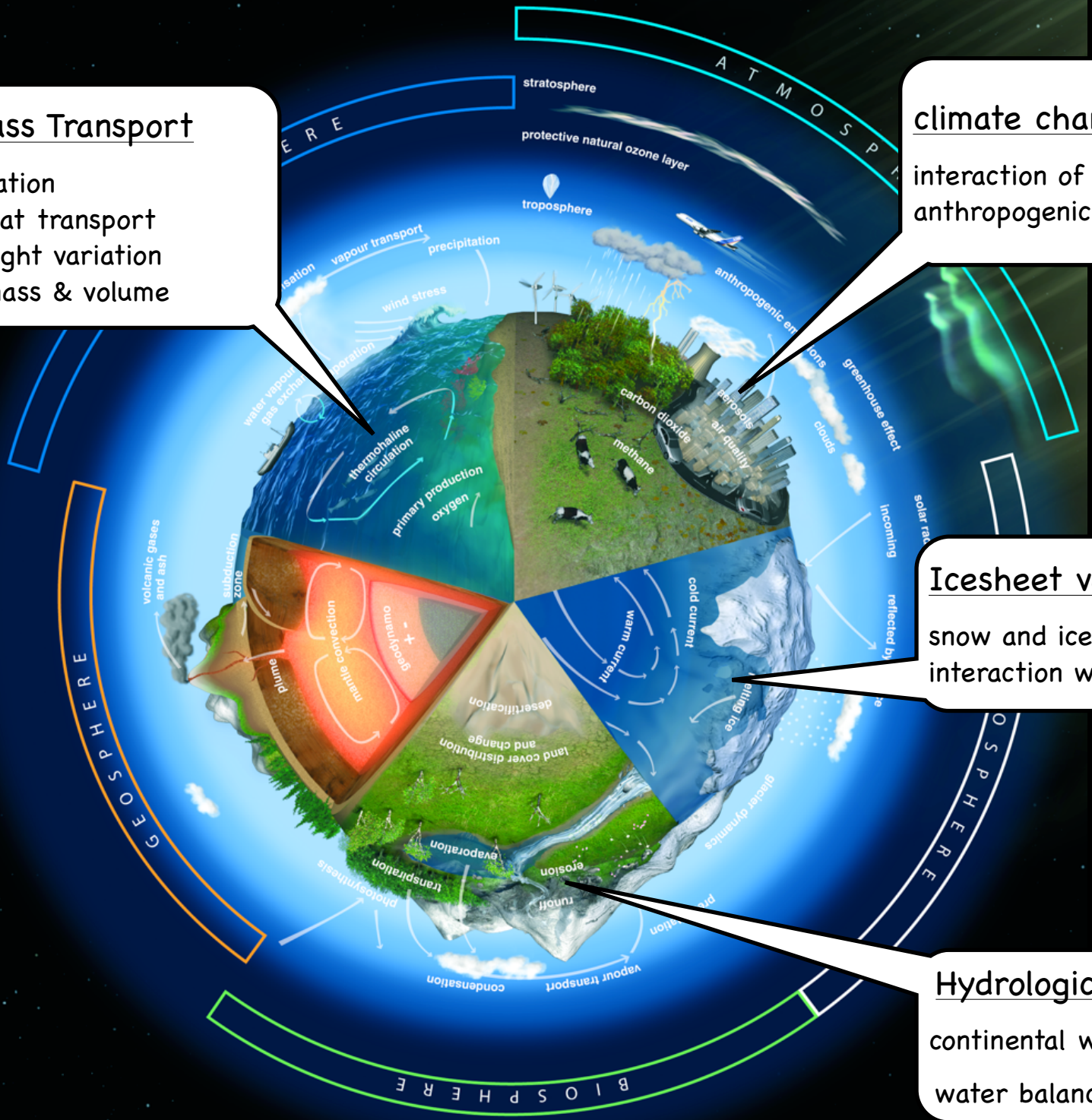

Icesheet variation

snow and ice coverage, dynamics
interaction with oceans

Hydrological Cycle

continental water budget

water balance (global/regional)

credits: ESA

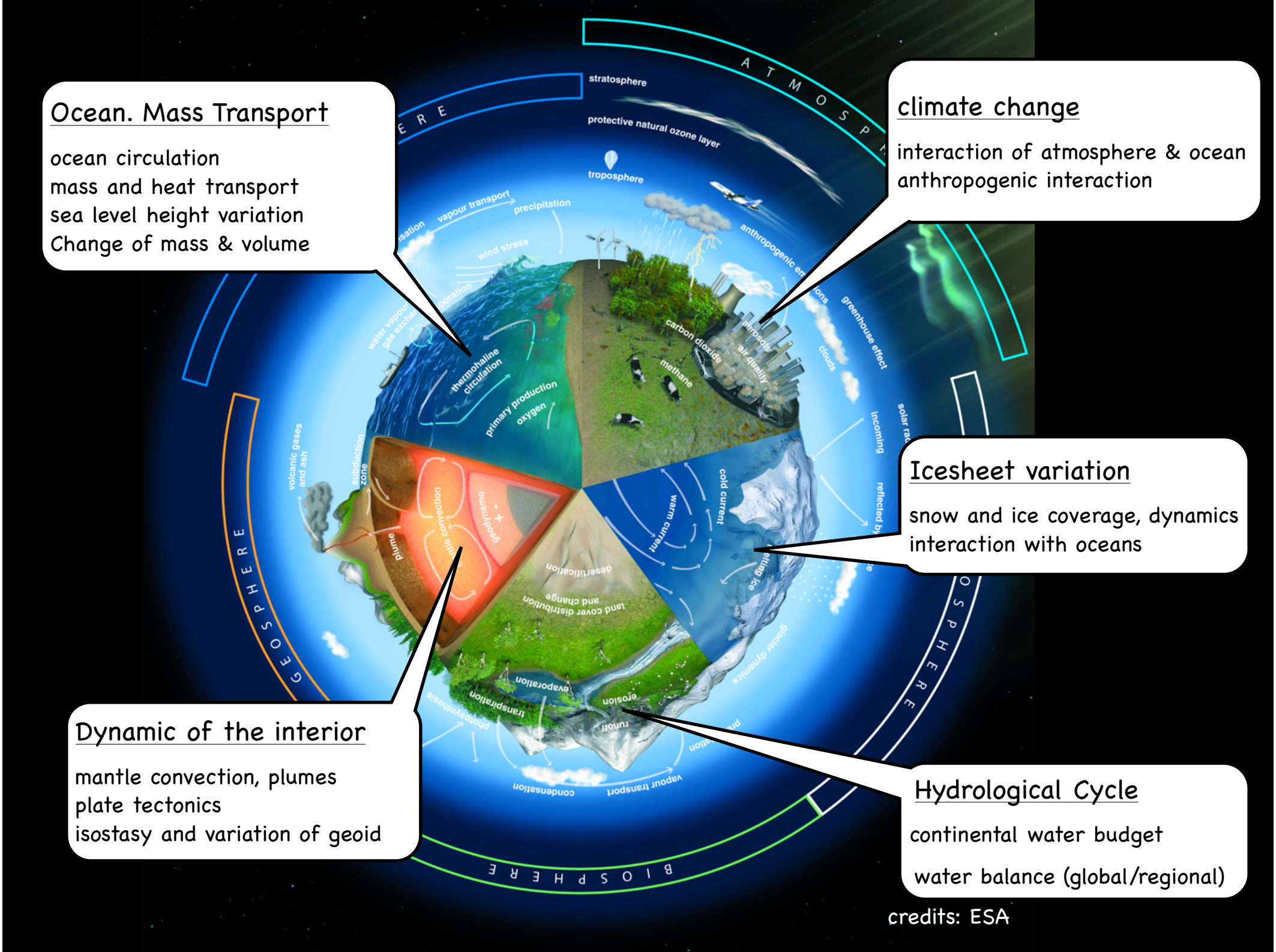
Ocean. Mass Transport
ocean circulation
mass and heat transport
sea level height variation
Change of mass & volume
climate change
interaction of atmosphere & ocean
anthropogenic interaction
Icesheet variation
snow and ice coverage, dynamics
interaction with oceans
Dynamic of the interior
mantle convection, plumes
plate tectonics
isostasy and variation of geoid
Hydrological Cycle
continental water budget
water balance (global/regional)
credits: ESA
stratosphere
protective natural ozone layer
troposphere
vapour transport
precipitation
wind stress
thermohaline circulation
primary production
oxygen
carbon dioxide
methane
aerosols
air quality
greenhouse effect
clouds
incoming
cold current
warm current
volcanic gases and ash
subduction zone
plume
geodynamo
desertification
land cover distribution and change
evaporation
transpiration
erosion
runoff
condensation
vapour transport
glacier dynamics
GEOSPHERE
BIOSPHERE

Ocean. Mass Transport

ocean circulation
mass and heat transport
sea level height variation
Change of mass & volume

climate change

interaction of atmosphere & ocean
anthropogenic interaction

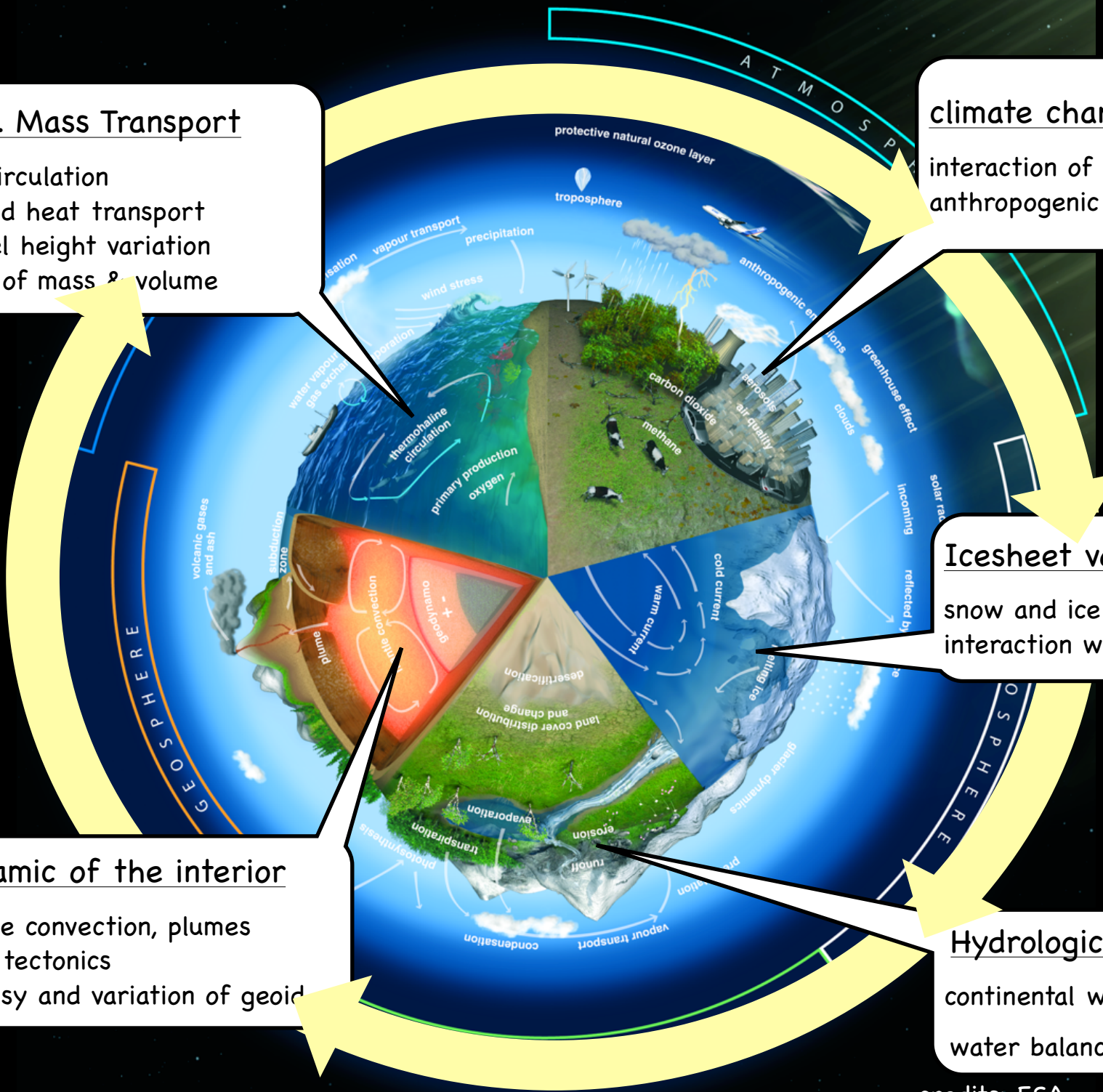

Icesheet variation

snow and ice coverage, dynamics
interaction with oceans

Dynamic of the interior

mantle convection, plumes
plate tectonics
isostasy and variation of geoid

Hydrological Cycle

continental water budget

water balance (global/regional)

credits: ESA

Intergovernmental Panel on Climate Change (IPCC)

modeled temperature scenarios

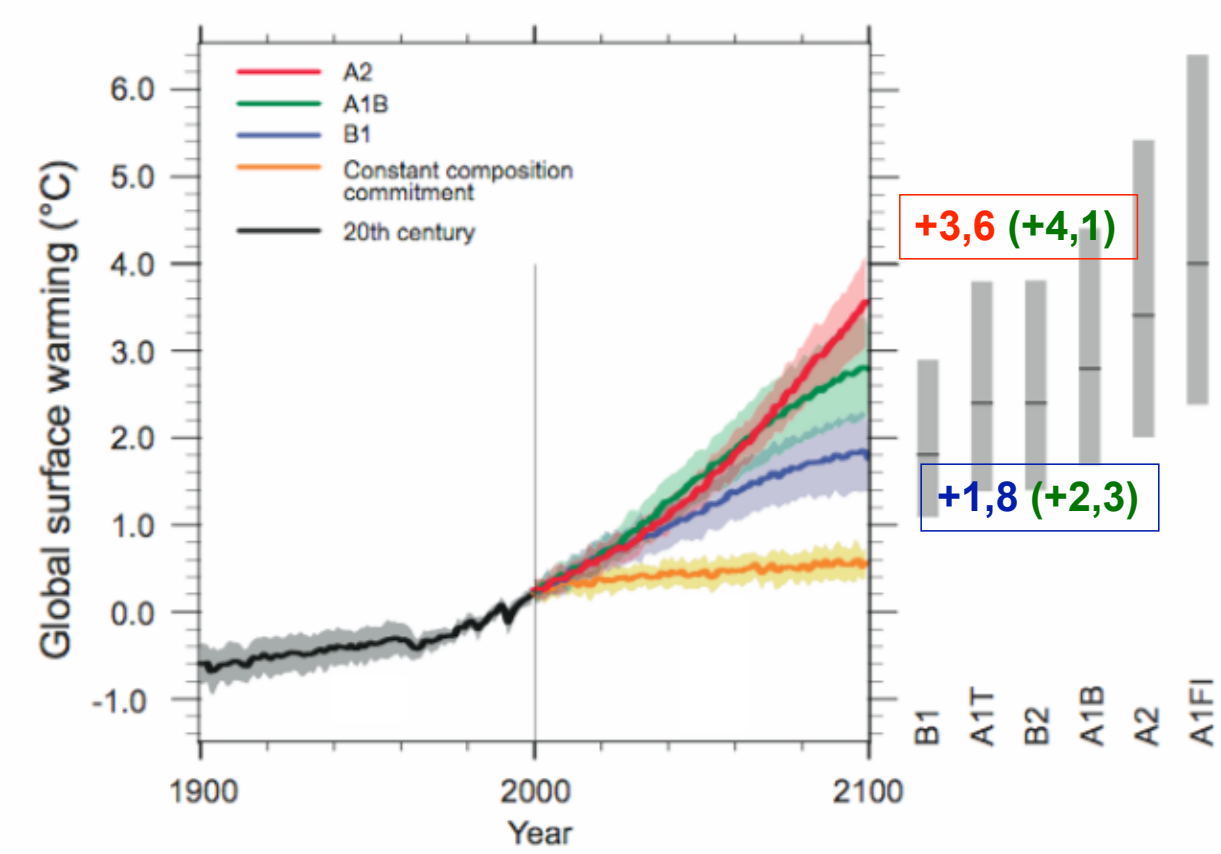

IPCC 2007

... examples

Increase in temperature → mean sea level rise

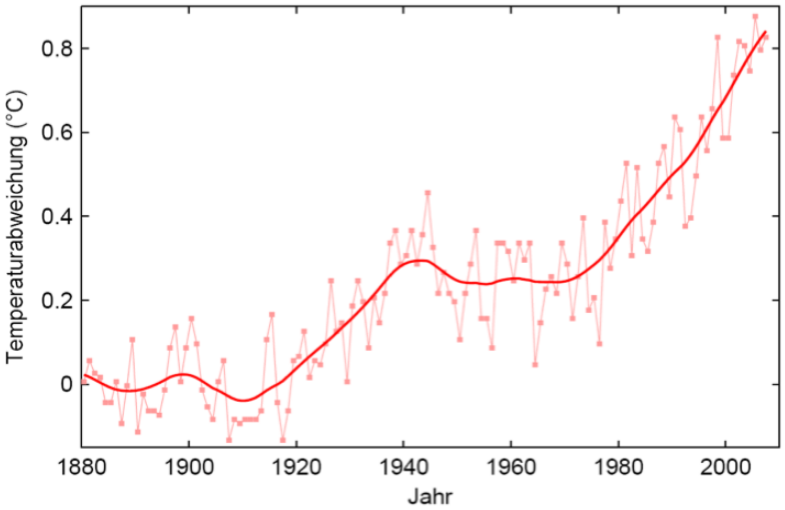

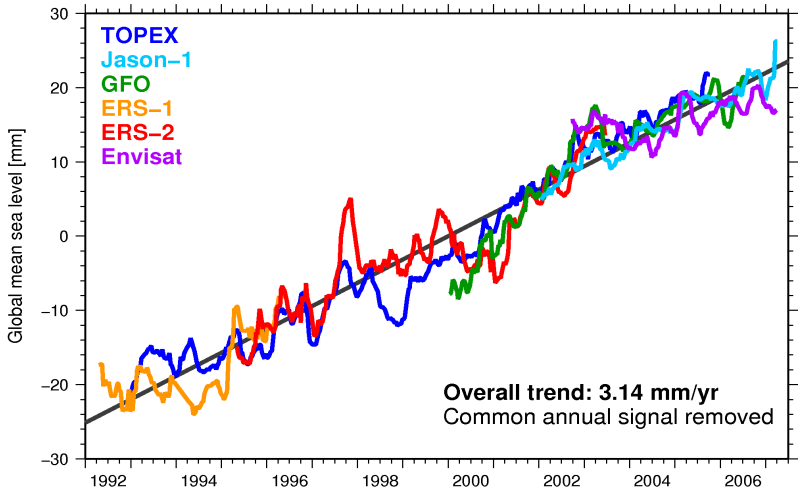

~0.8°C in the last century

~20 cm over the last century

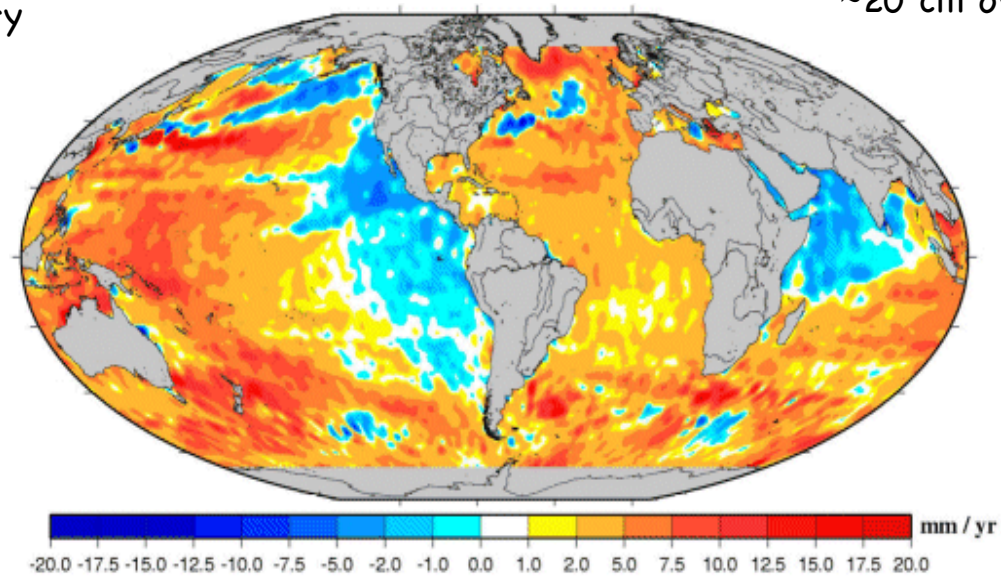

GRACE – Results: Greenland

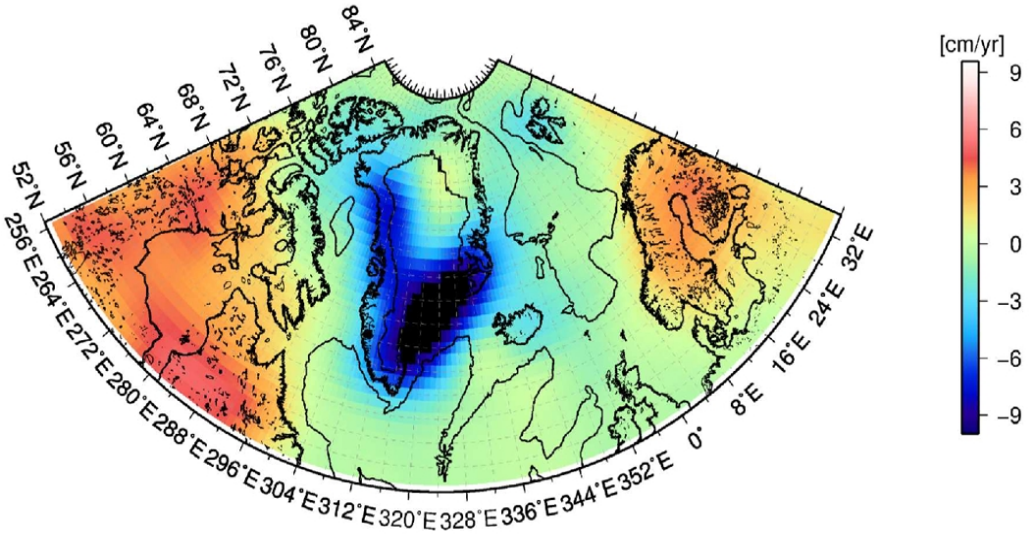

Variation (equivalent water height) in Greenland (Feb. 2003 – Jan 2009) derived from GRACE

(Wouters et al., 2008)

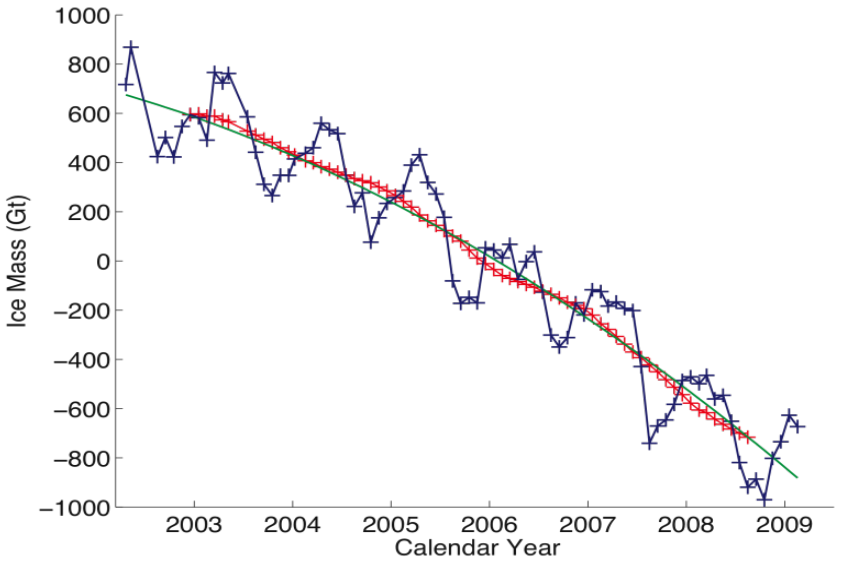

→ approx. 180 Gt per year

(Velicogna et al, 2009)

Plate Tectonics → Earthquakes

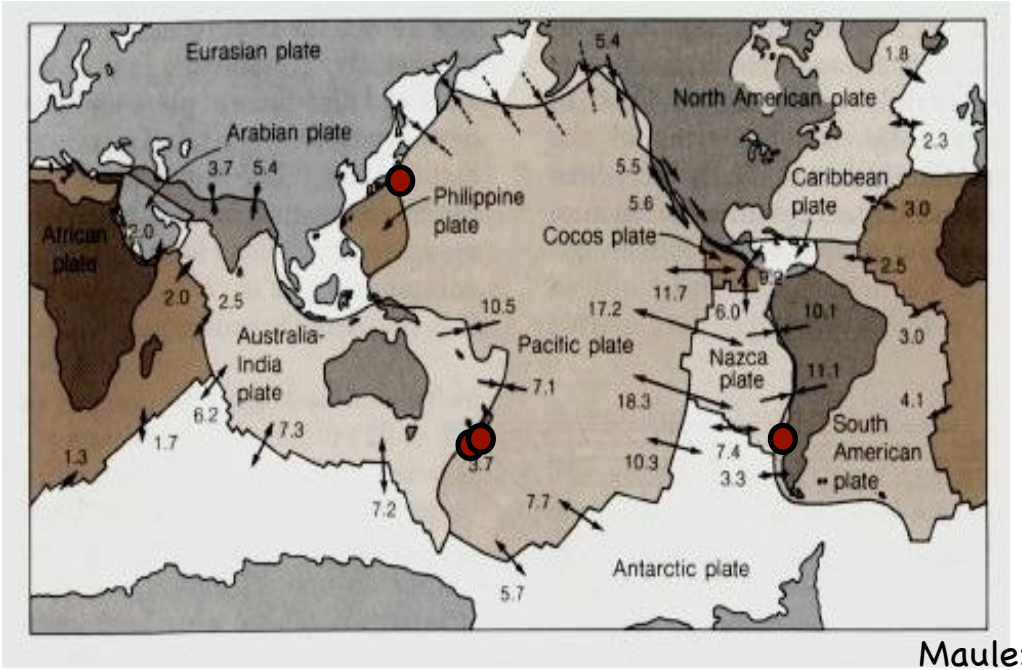

recent examples:

Maule: 27.2.2010 (mag. 8.8)

ChCh: 2.9.2010 (mag. 7.4)

ChCh: 22.2.2011 (mag. 6.3)

Japan, 11.3.2011 (mag. 9.0)

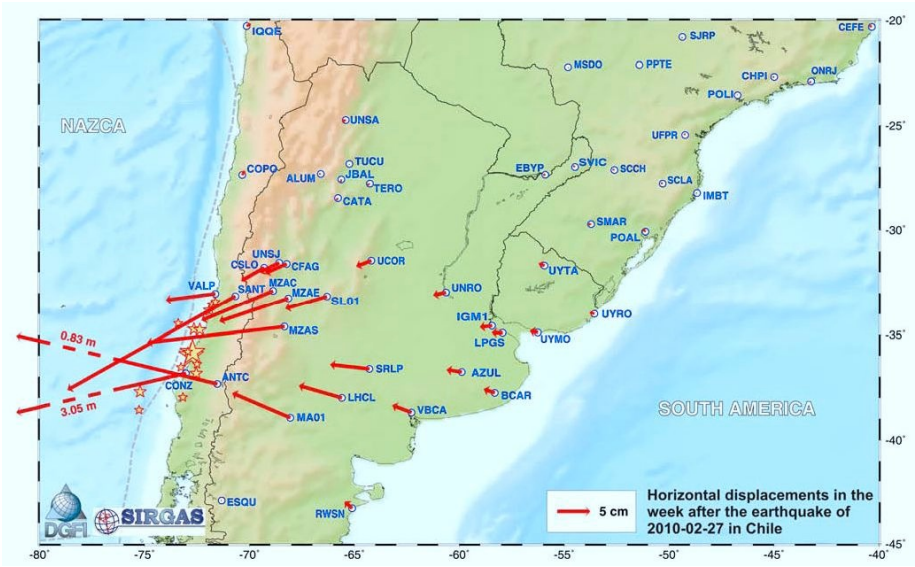

System Earth - Relevant Timescales

Lithosphere:

Plate Tectonics ↔ Earthquakes

Millions of Years ↔ several Seconds

cm/year ↔ km/s

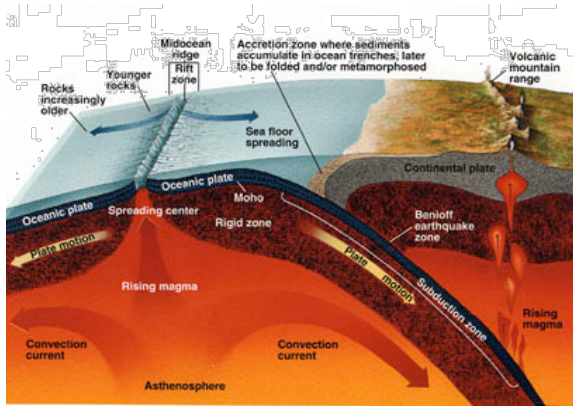

Hydrosphere:

Sea Level Rise ↔ Tsunami

3 mm/year ↔ 300 m/s

Atmosphere:

Climate ↔ Weather

years - decades ↔ hours - days

→ Requirements

Measurement techniques of extremely high resolution and stability

Quantification of very small and slow processes vs. highly dynamic realtime

➢ „Internal" Goal

Evolution of GGOS and the geodetic observation technologies to establish an Earth fixed reference frame with a relative accuracy of at least

10^{-9} = 1 ppb

with high spatial and temporal resolution.

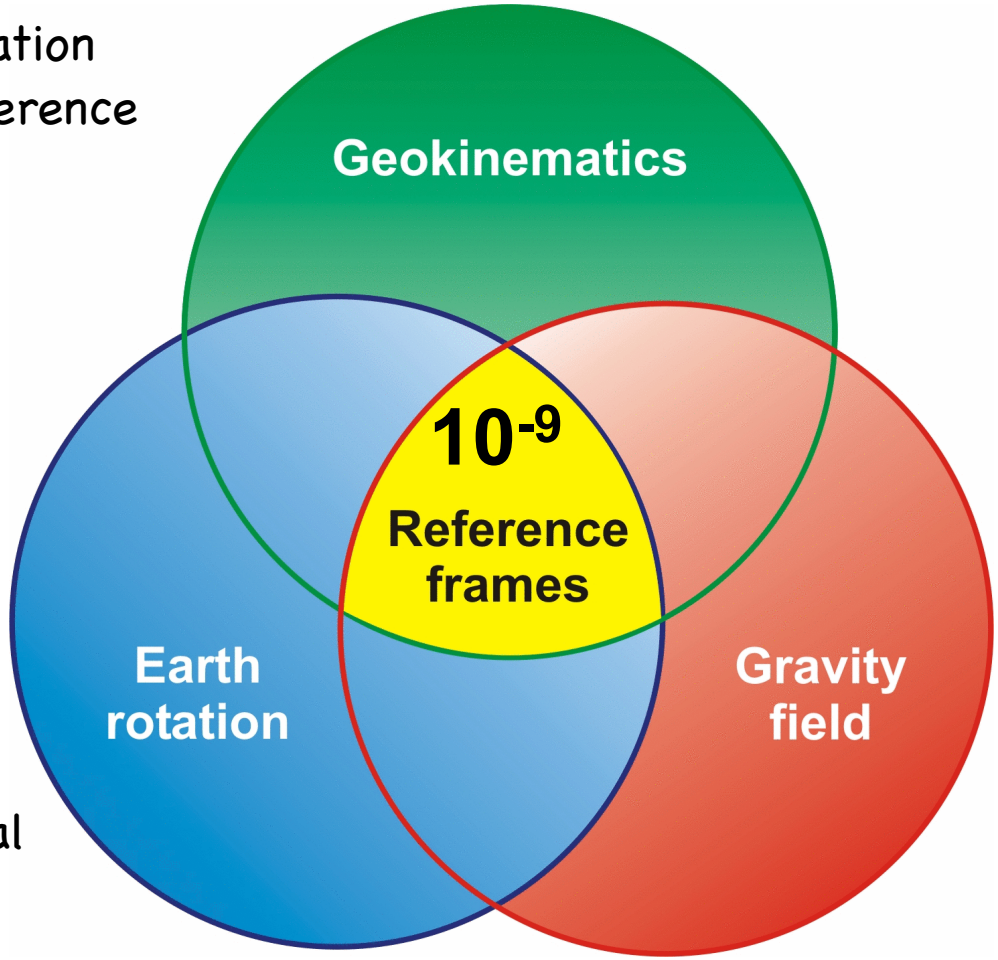

➢ „External" Goal

Integration of GGOS as an important contributor into **Earth System Research** (Modeling of physical, chemical and biological processes).

Contributions: Mass transport, dynamics, surface deformations.

Earth rotation as the link between ICRF and ITRF

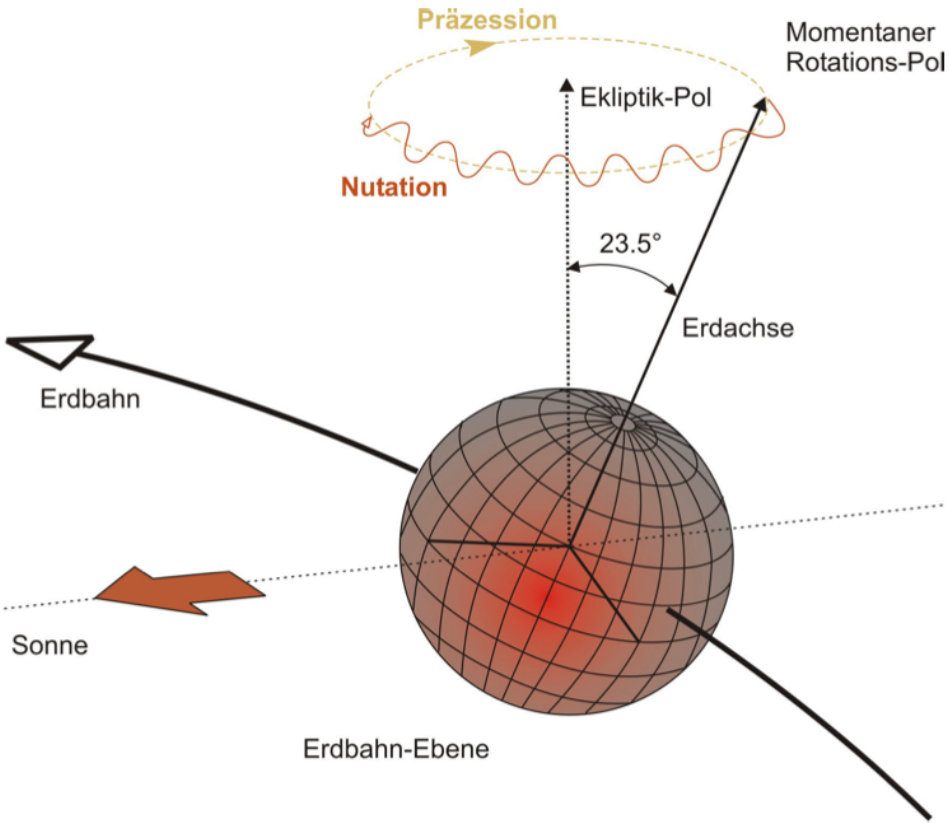

a) the rotation rate of the Earth is not constant. Deceleration by dissipation and variation by momentum exchange. Free oscillations excited by ocean, atmosphere

b) gravitational attraction of sun and moon on a near spherical object give rise to precession and nutation

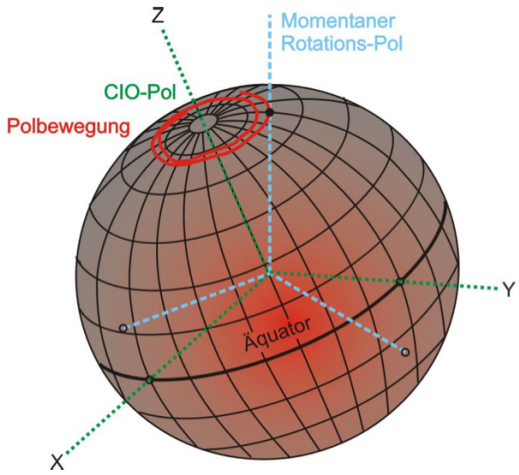

c) mass redistribution on Earth and the fact that the figure axis and the axis of Inertia are not coinciding, give rise to polar motion

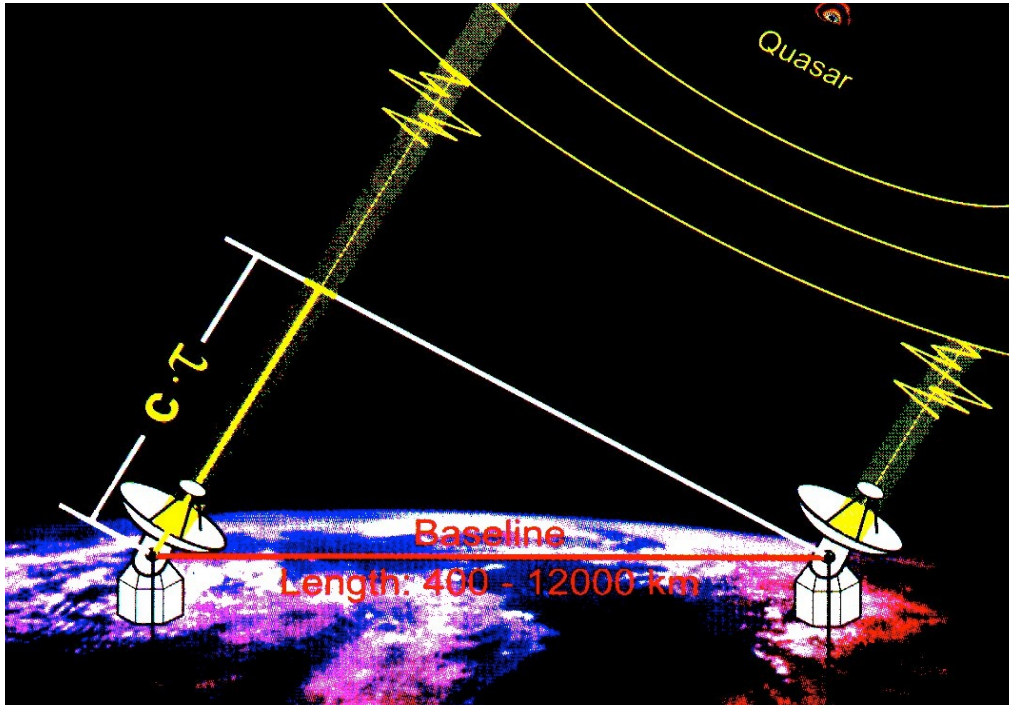

Very Long Baseline Interferometry

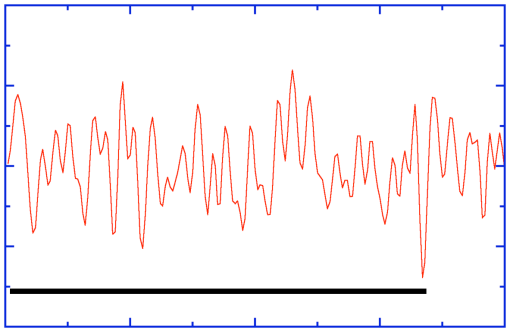

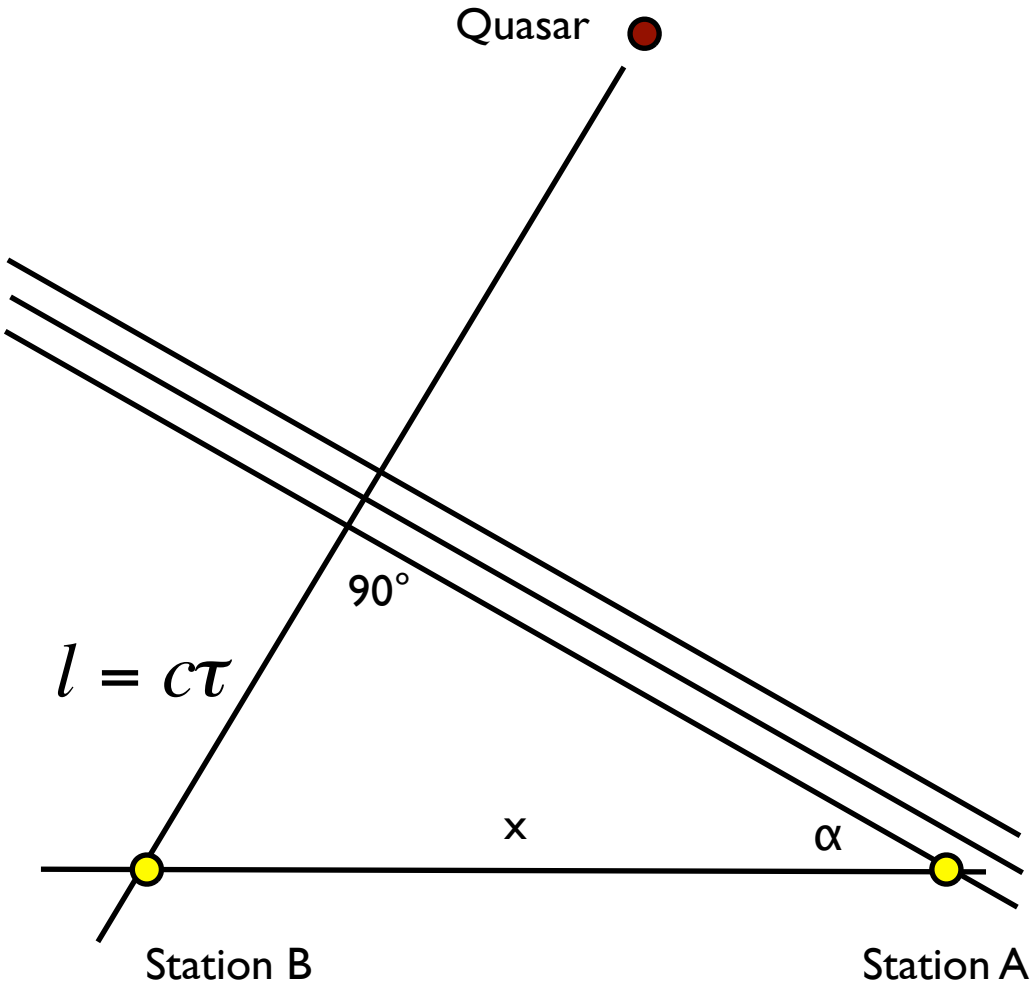

$$l = c\tau$$

$$\sin\alpha = \frac{l}{x}$$

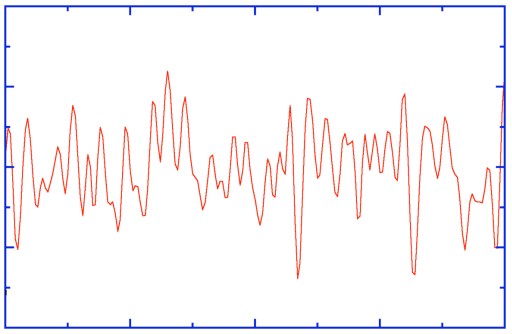

Sagnac Interferometer (1913)

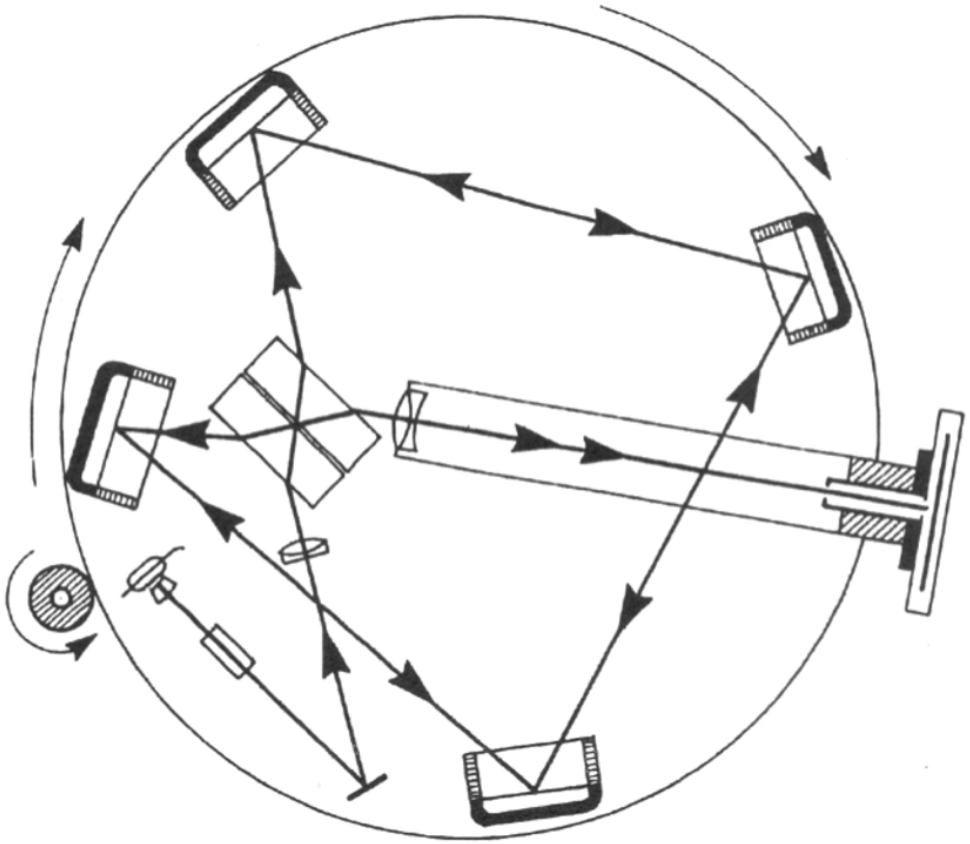

Rotation Rate: 2 rev. per sec.

observed Fringe Shift:

$$\delta\phi = \frac{8\pi A}{\lambda c}\boldsymbol{n}\cdot\boldsymbol{\omega}$$

with A = 0.086 m^2 this turns out to be 0.07±0.01 fringes

Georges Sagnac was the first to correctly combine theory with experiment. We also acknowledge the experimental skill to build a sufficiently stable apparatus.

The Michelson - Gale Interferometer in Clearing, Illinois (1925)

(upscaling provided a fringe pattern solely caused by Earth rotation)

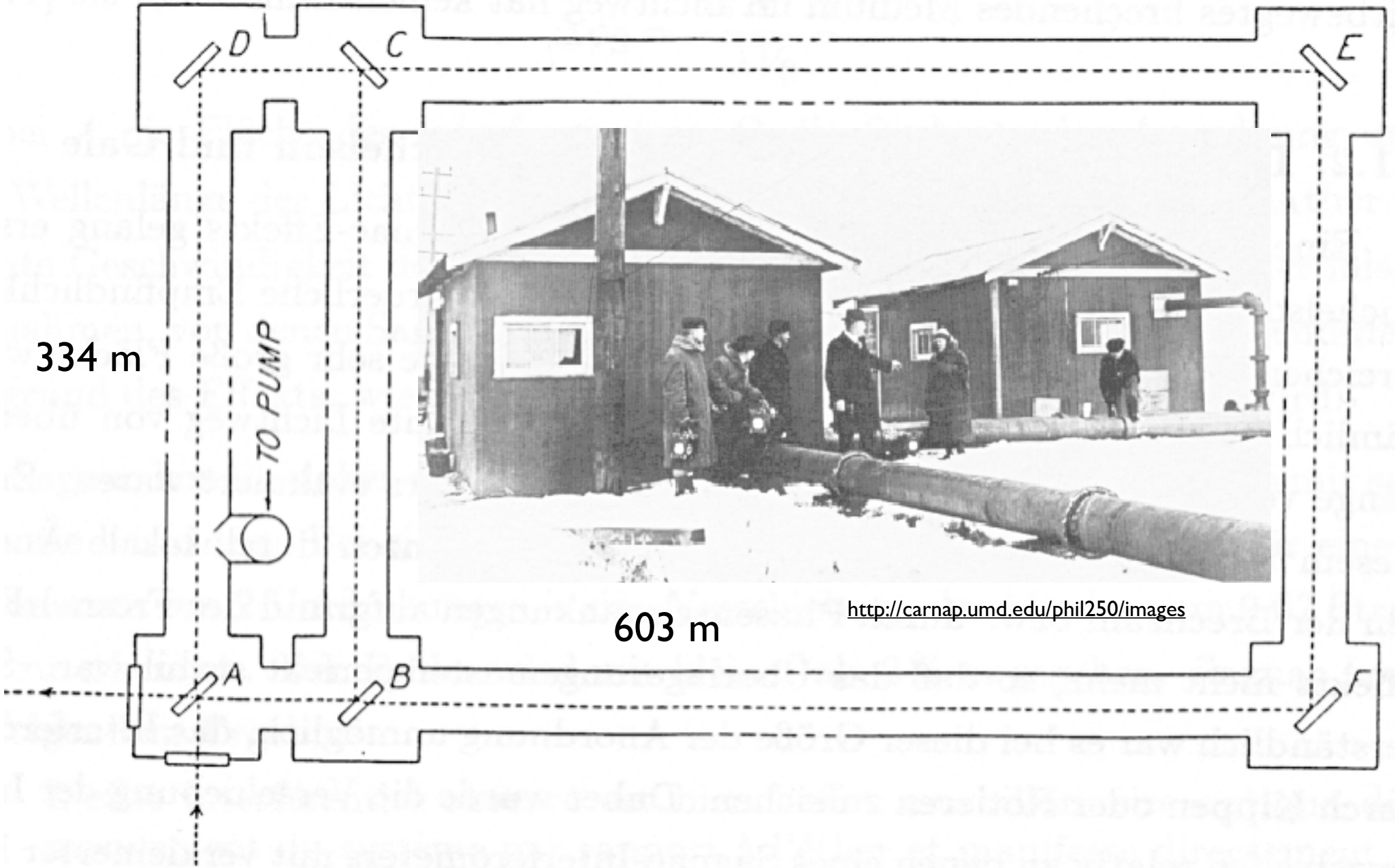

http://carnap.umd.edu/phil250/images

The Michelson - Gale Interferometer in Clearing, Illinois (1925)

(upscaling provided a fringe pattern solely caused by Earth rotation)

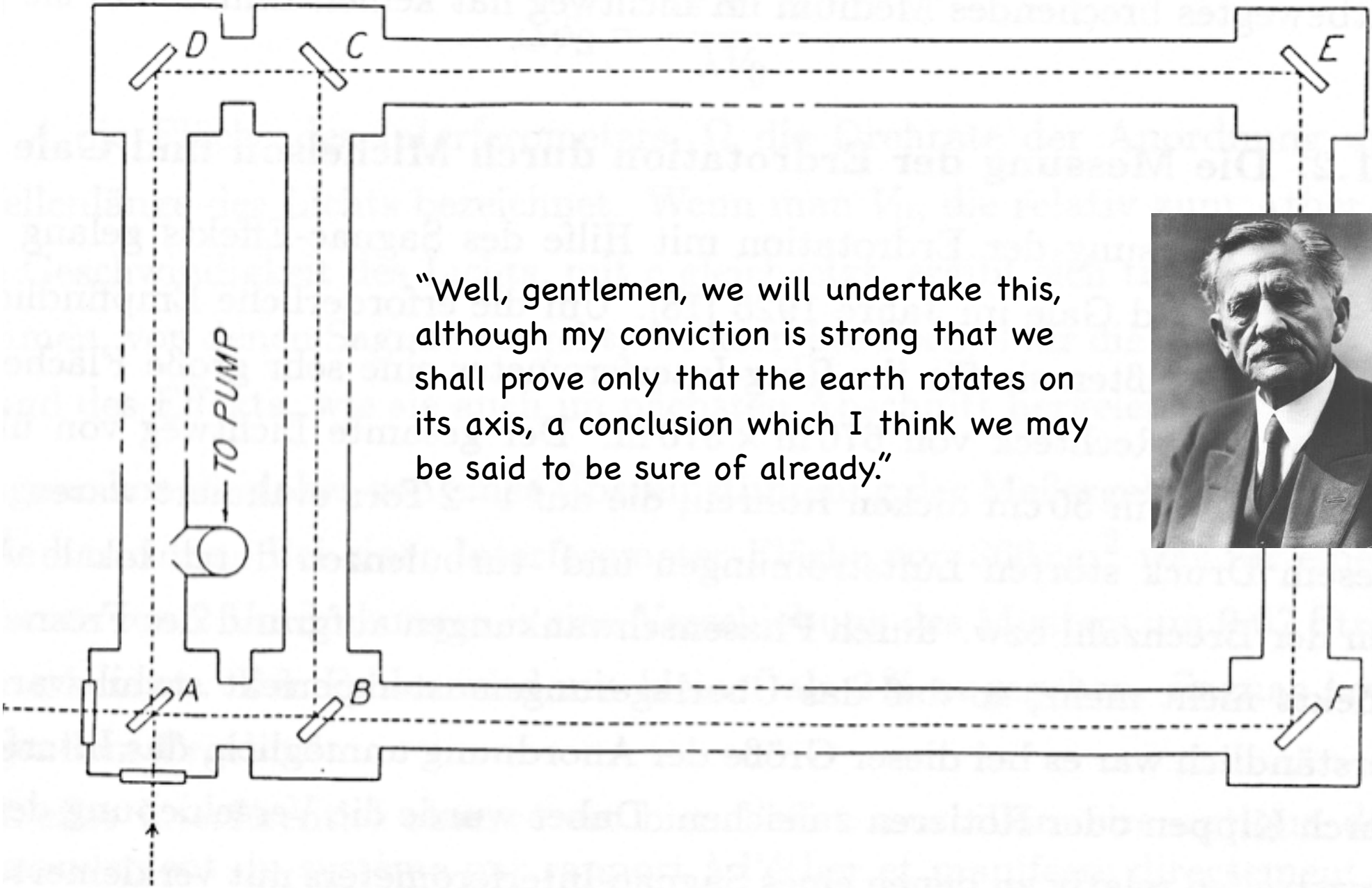

"Well, gentlemen, we will undertake this, although my conviction is strong that we shall prove only that the earth rotates on its axis, a conclusion which I think we may be said to be sure of already."

Shortly after the successful demonstration of an optical maser, rotation sensing with active optical interferometers have been pursued...

Volume 2, Number 3 APPLIED PHYSICS LETTERS 1 February 1963

ROTATION RATE SENSING WITH TRAVELING-WAVE RING LASERS

W. M. Macek and D. T. M. Davis, Jr.
Sperry Gyroscope Company
Division of Sperry Rand Corporation
Great Neck, New York

(Received 15 January 1963)

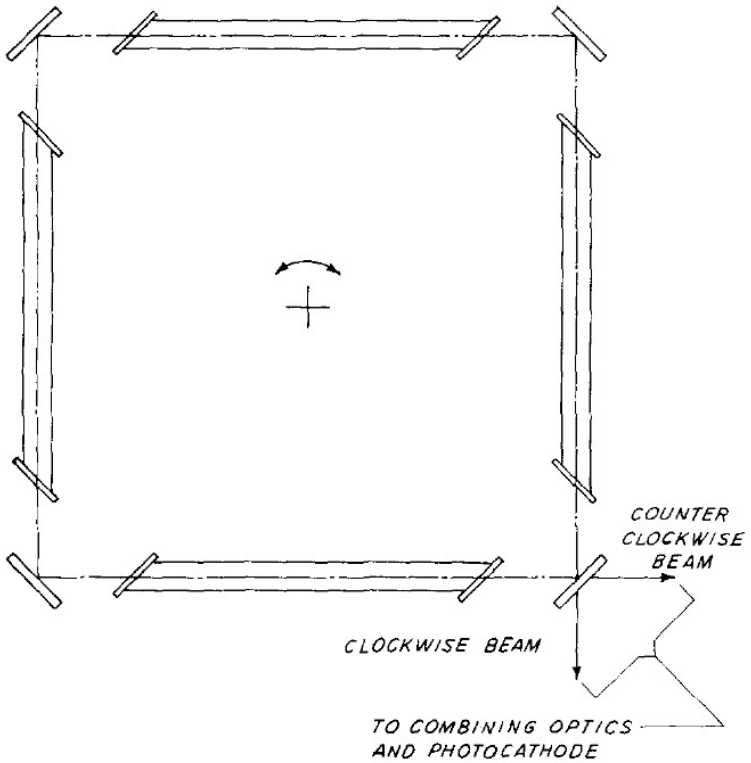

The sensing of rotation rate with respect to an inertial frame of reference has been demonstrated using a cw He-Ne gas traveling-wave ring laser, shown schematically in Fig. 1. The 1.153-μ line of the He-Ne gas system was employed with a meter-square laser ring resonator. Four gas tubes were used with Brewster angle windows and four external corner mirrors. Since the cw oscillation is obtained

While the first laser gyro did not unlock on the rotation rate of the Earth and had to be spun to demonstrate gyroscope functions...

...a rapid development process made them a preferred instrument for navigation over the the course of the 70's

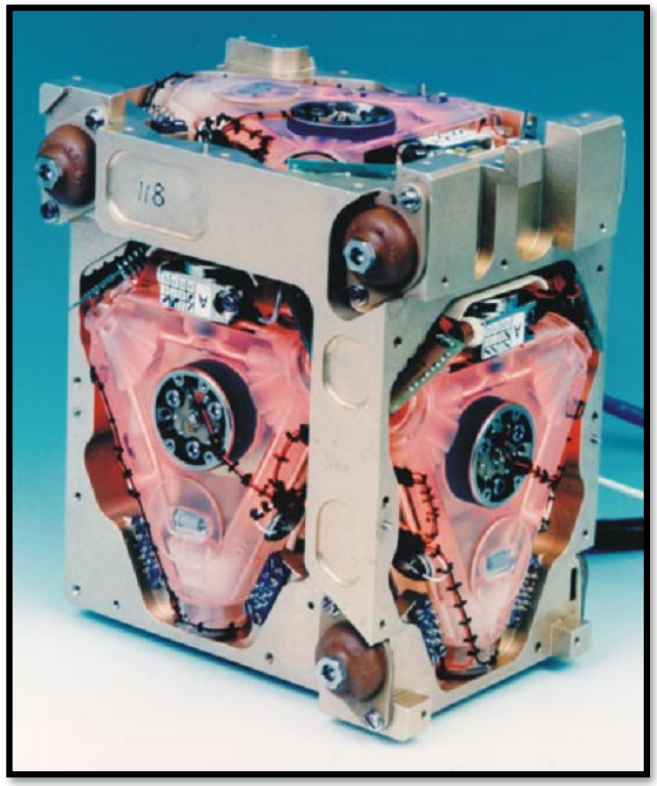

Geodesy provided the motivation to renew the development of ring lasers

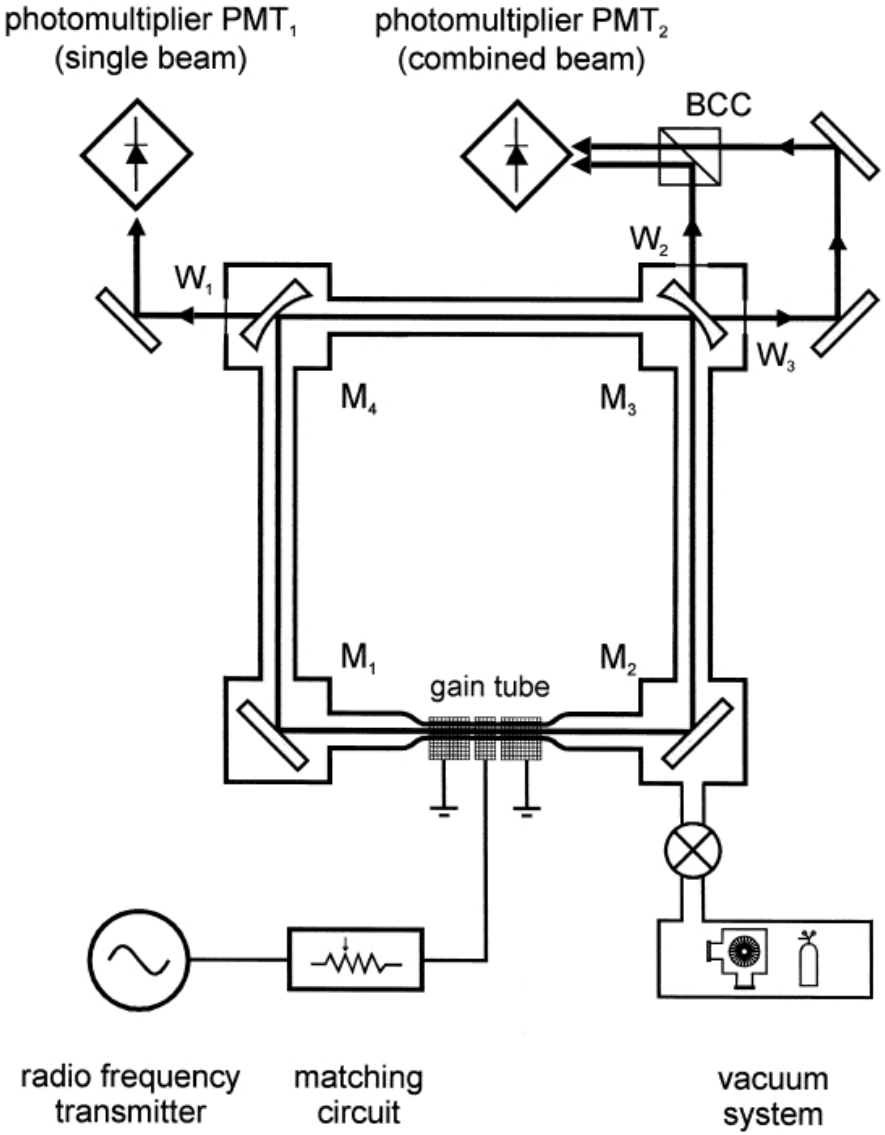

Since Earth rotation is the link between the global terrestrial and the celestial reference frame, Sagnac interferometry was considered a promising approach for a constant monitoring

Significant upscaling provides the necessary 9 orders of magnitude dynamic range

Gravitational wave detection technology development eventually delivered suitable mirrors to combat lock-in at the Earth rate

$$\delta f = \frac{4A}{\lambda P}\,\vec{n}\cdot\vec{\Omega} + f_{nr}$$

$10^{-9}\Omega_E \approx 0.07$ prad/s

Baseline: monolithic Gyro Design

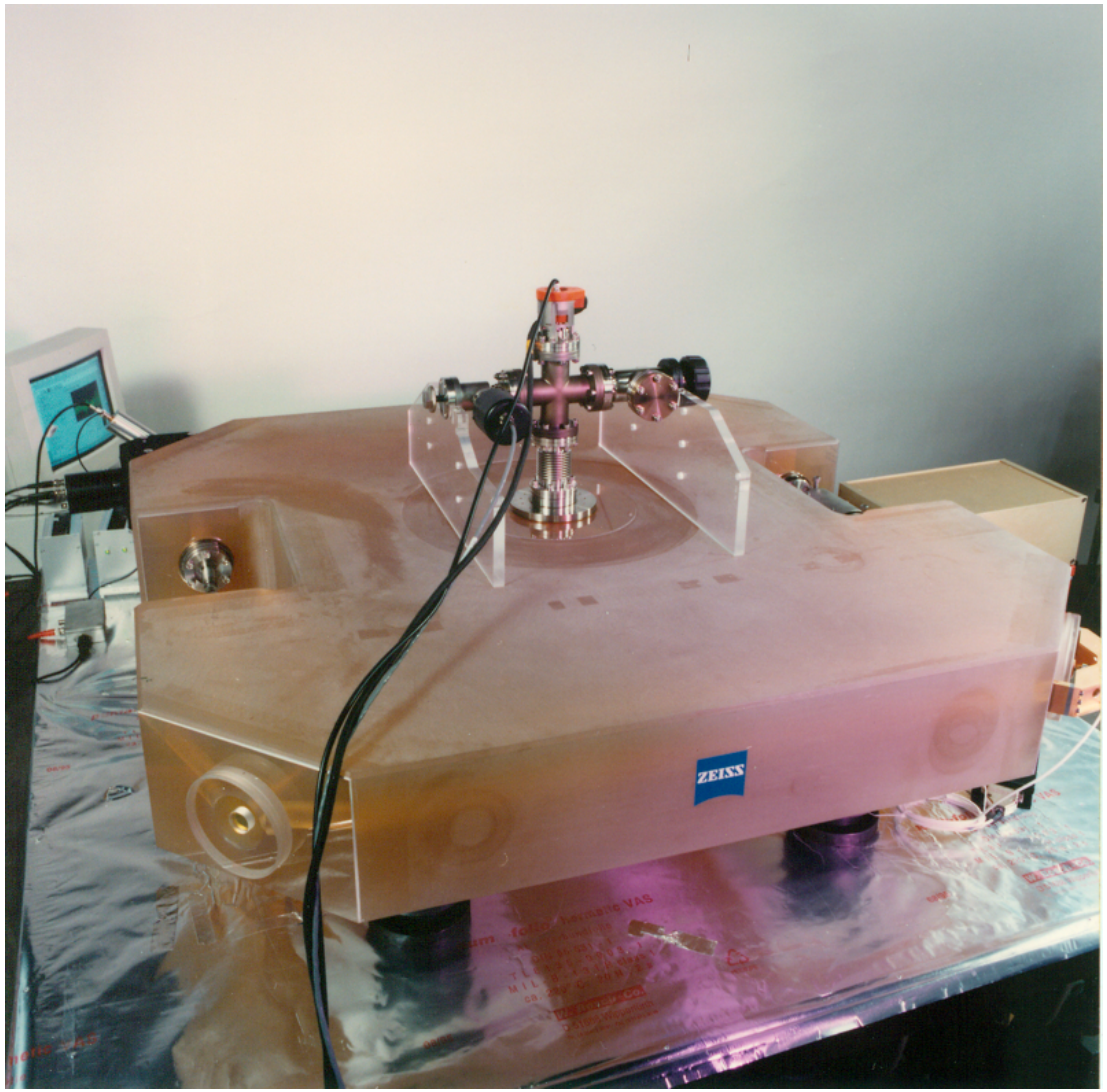

- Prototype: C-II (1997)
- Perimeter 4 m
- He-Ne (632.8 nm)
- Cavity in Neutral Plane
- UHV-Compatibility
- RF-Excitation

Feasibility of Project shown

Alternative Concept: UG-2 RLG with 834 m^2 of Area

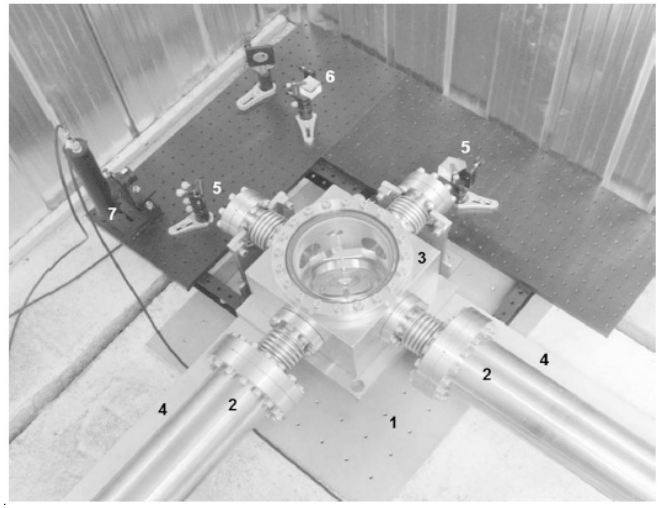

UG-2 built in 2003 with dimensions: 39.7 m x 21 m
Heterolithic concept built from stainless steel tubes

Scale Factor Variations in UG-2 inferred from Beam Wander Measurements

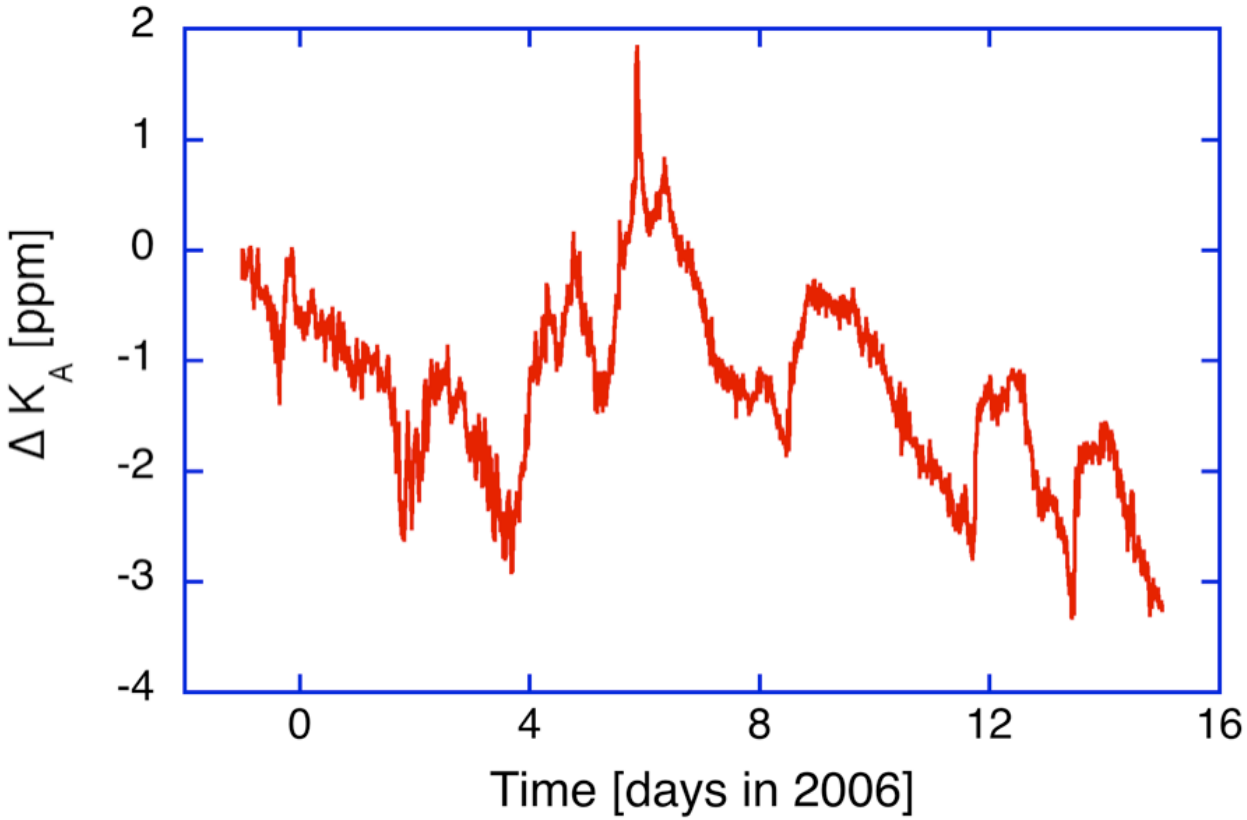

Long term stability is in the ≈ 5 ppm regime with a short term stability much worse

G - Ring the currently best performing gyro

- Perimeter: 16 m
- Area: 16 m^2
- FSR 18.75 MHz
- $\Delta \nu_L \approx 274\ \mu Hz$
- 5 ppm total loss
- $Q = \omega \tau \approx 5 \times 10^{12}$

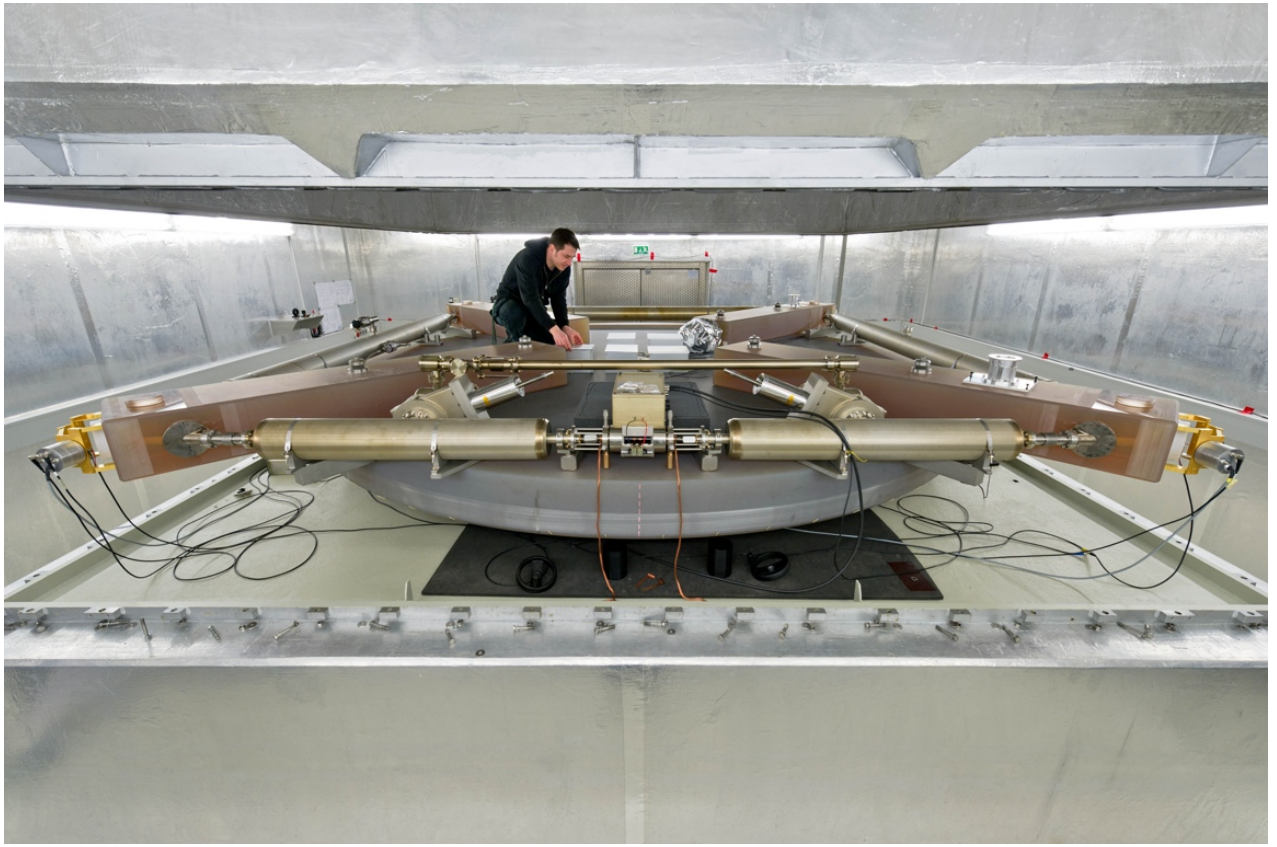

- 6.5 mB gas pressure in order to avoid multi-moding

A typical timeseries of G ring laser measurements...

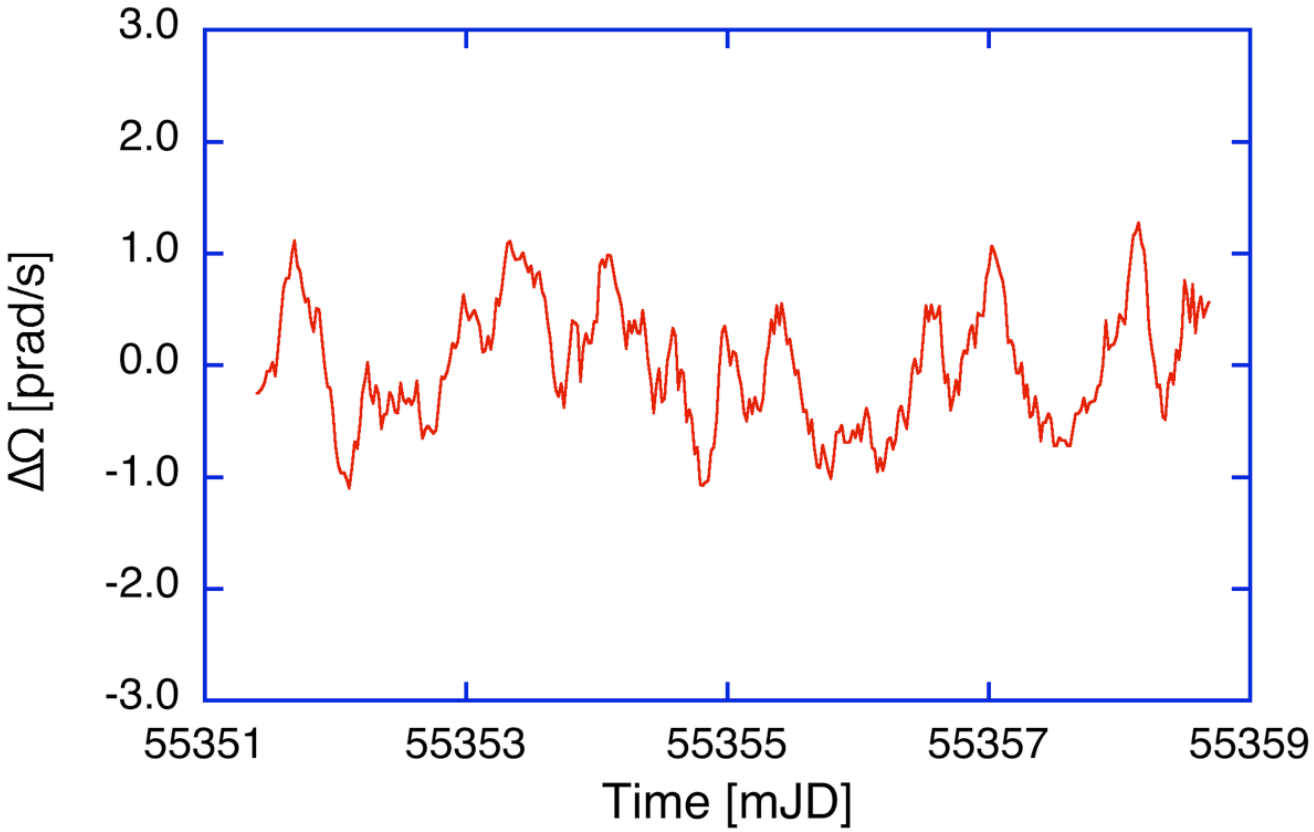

... containing not modeled external signals and sensor noise (most prominently backscatter contributions)

Geodetic Observatory Wettzell

Stability chart of our important large gyros

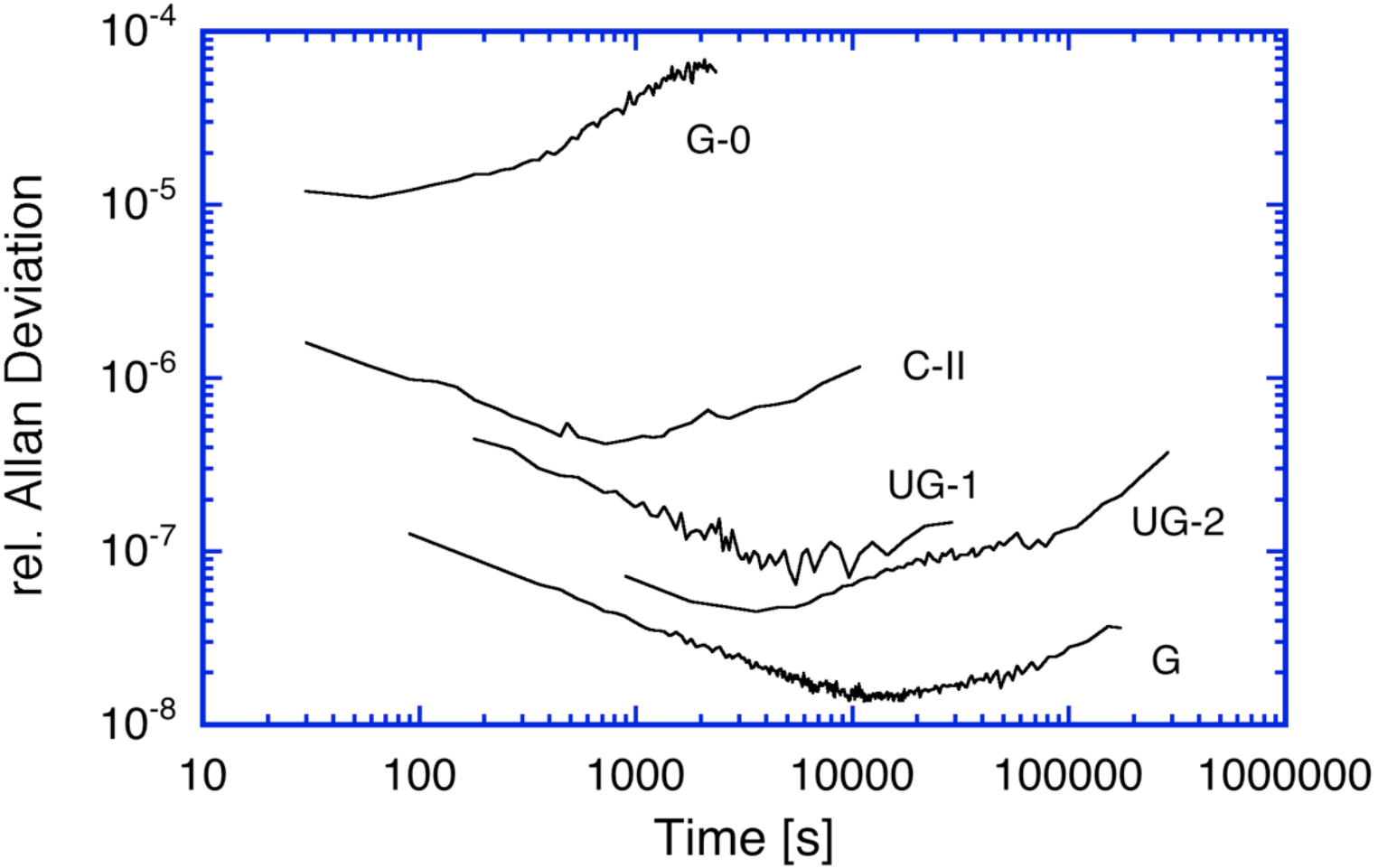

Operations can be stabilized by controlling the perimeter via a pressure stab. vessel

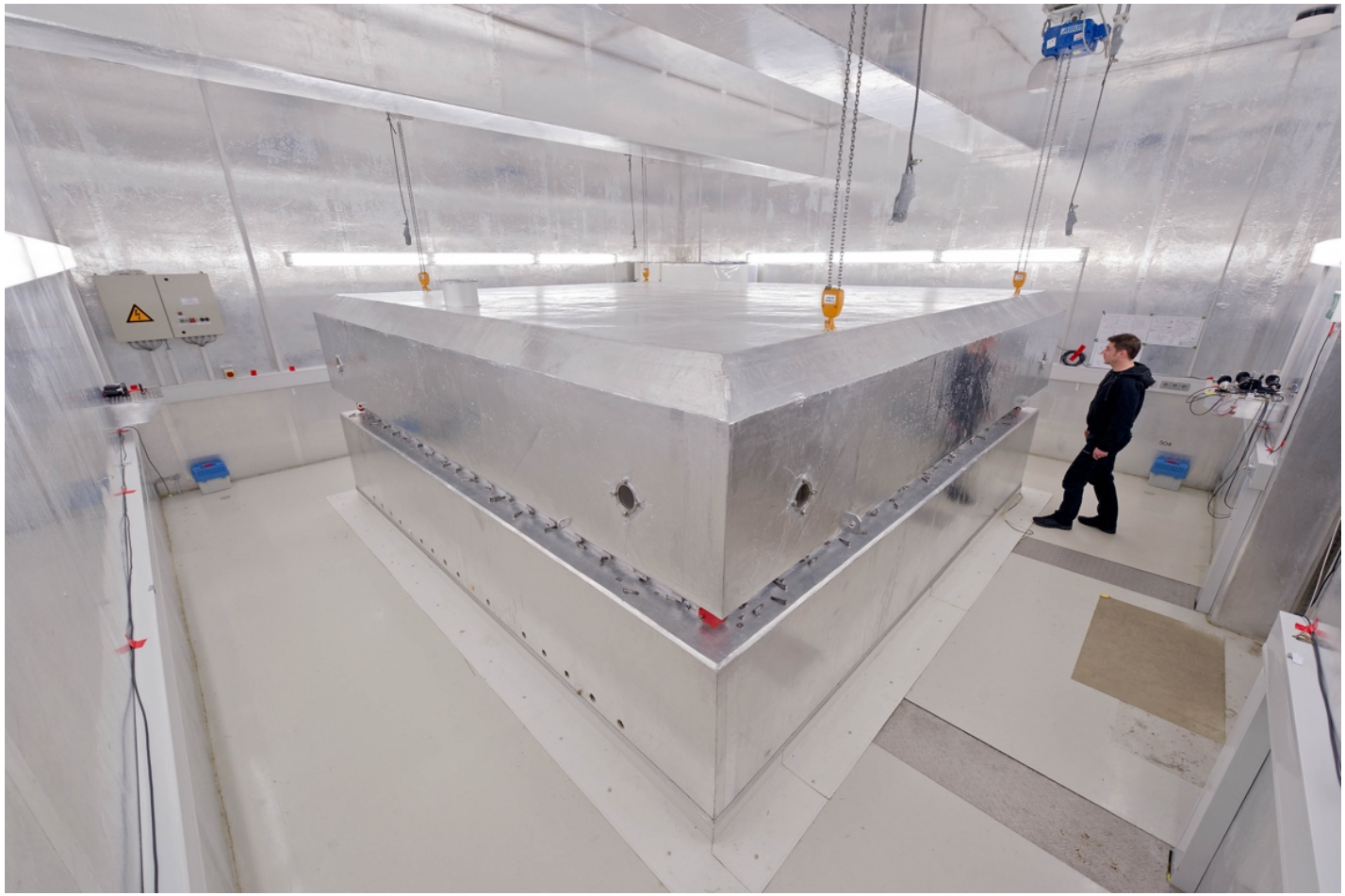

Comparison of G tied to the Earth crust against the (known) geophysical signals due to orientation variation

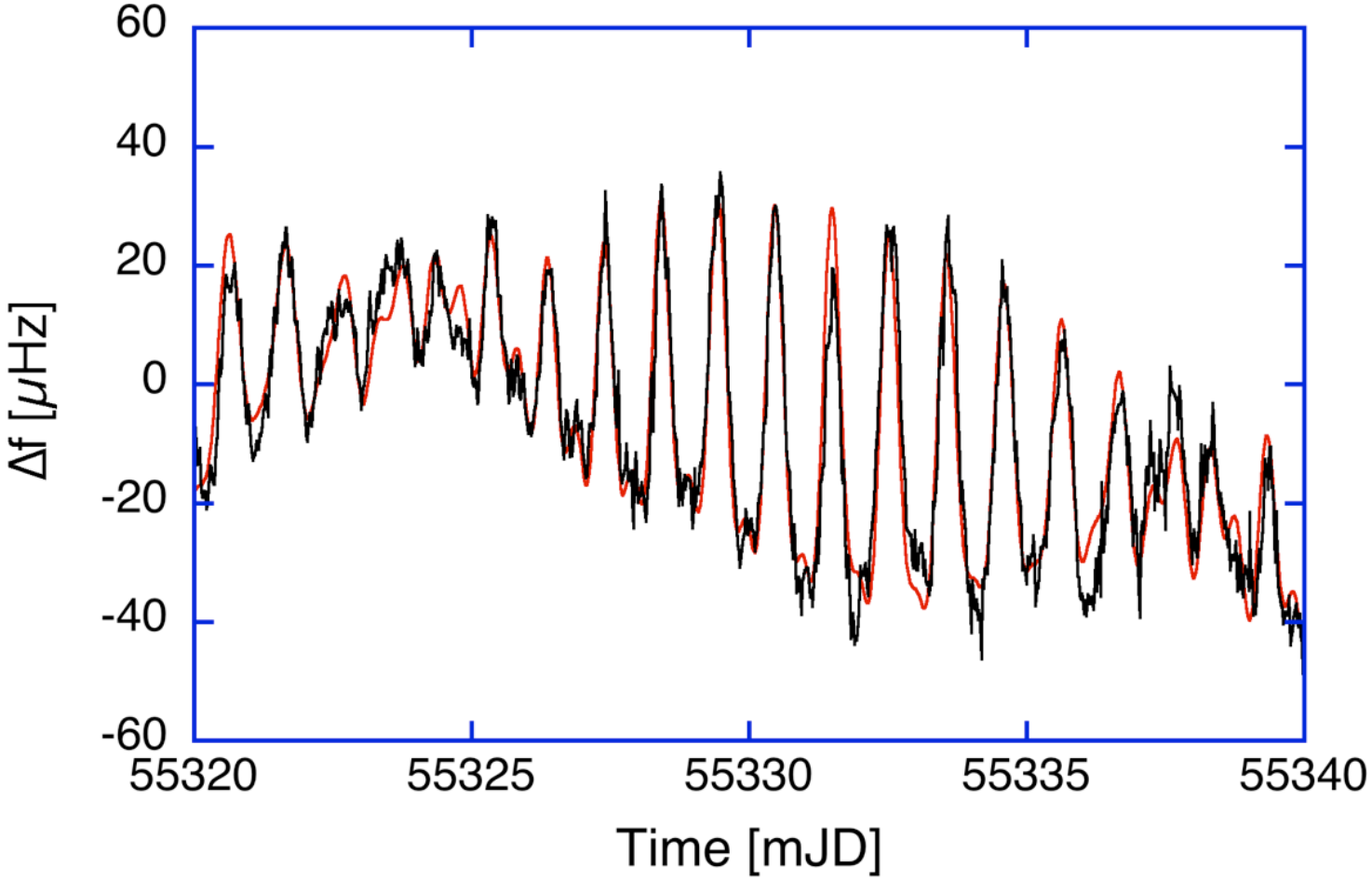

Earth rotation causes a beat note of 348.522 Hz. Tilt induced geophysical signals show signatures in the range of ±0.000050 Hz

… the Chandler and the annual wobble

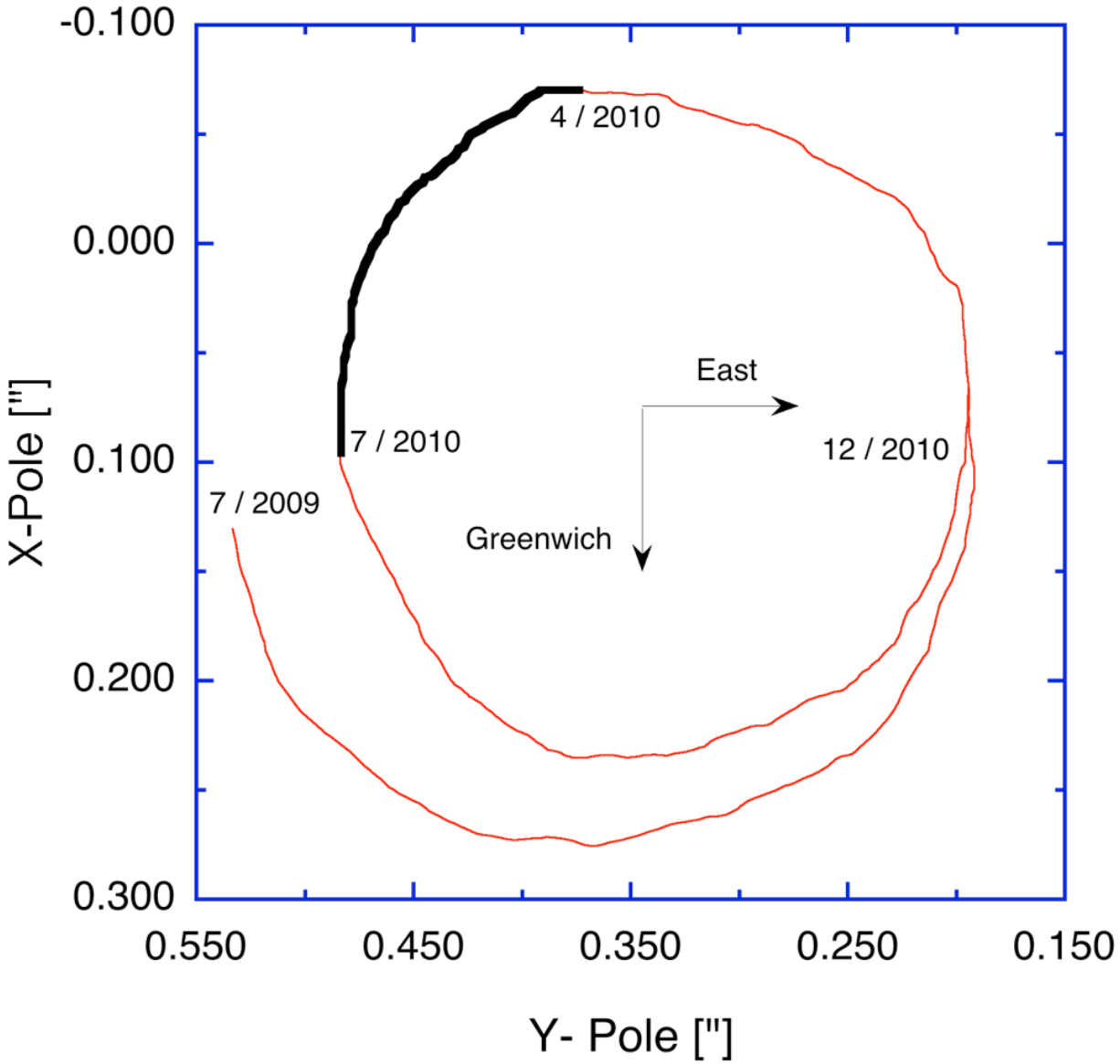

Comparison to VLBI measurements

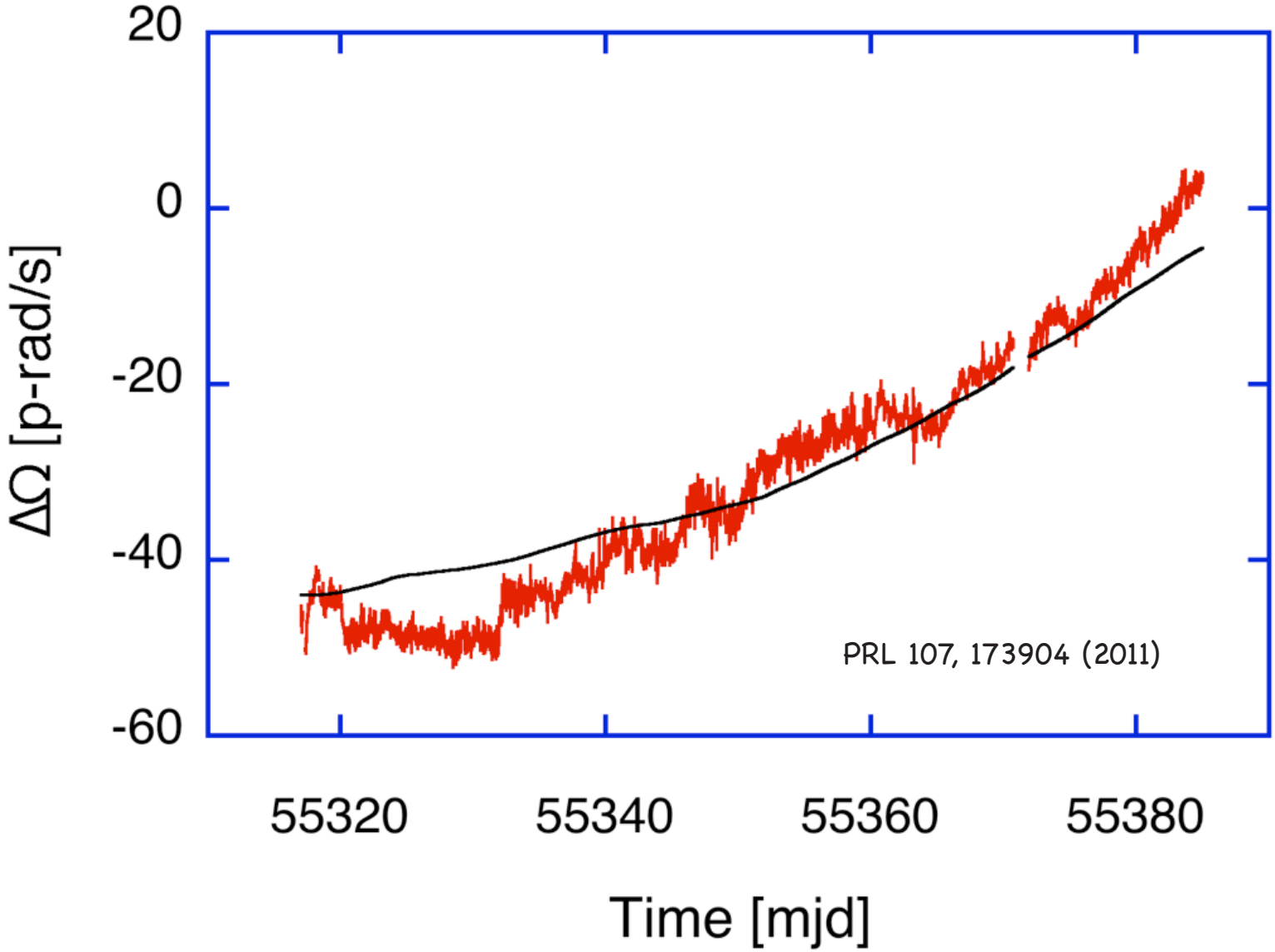

Interim Summary:

$$\delta\Omega = \frac{cP}{4AQ}\sqrt{\frac{hf}{P_x t}}; \qquad \delta\Omega = 1.2\times10^{-11}\,\frac{\text{rad}}{\text{s}\sqrt{\text{Hz}}}$$

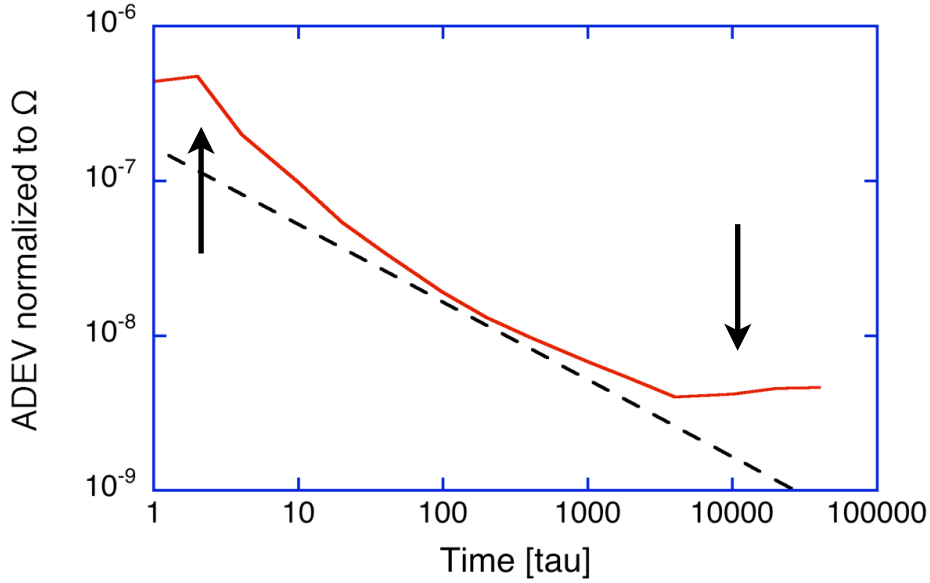

- Sensitivity sufficient
- limited by micro seismics for short integration times
- limited by stability for long integration times (backscatter)

Plane transversely polarized wave propagating in x-direction with phase velocity c

$$u_y(x,t) = f(kx - \omega t) \qquad c = \omega / k$$

Acceleration $$a_y(x,t) = \ddot{u}_y(x,t) = \omega^2 f''(kx - \omega t)$$

Rotation rate $$\dot{\Omega}(x,t) = \frac{1}{2}\nabla \times \left[0, \dot{u}_y, 0\right] = \left[0, 0, -\frac{1}{2} k\omega f''(kx - \omega t)\right]$$

$$\longrightarrow \quad a(x,t) / \dot{\Omega}(x,t) = -2c$$

Rotation rate and acceleration should be in phase and the amplitudes scaled by two times the horizontal phase velocity

Rotations in Seismology:

For plane transversely polarized waves we find from theory:

Rotation rate and acceleration are in phase and the amplitudes scale by two times the horizontal phase velocity:

$$a(x,t) / \dot{\Omega}(x,t) = -2c$$

This applies for earthquake signals as well as for microseismic activity

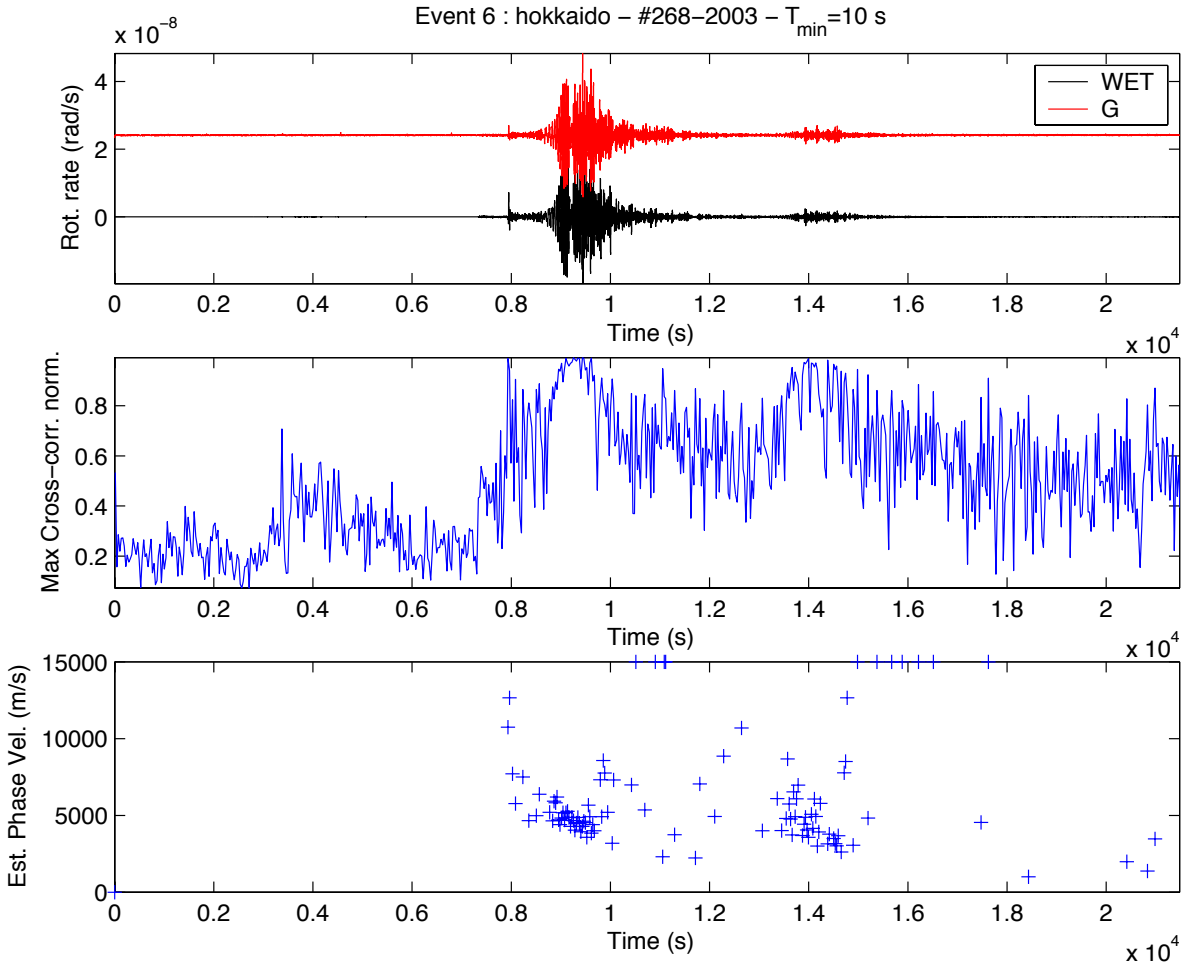

Ring Laser and Seismometer Data is filtered at the Frequency Band of the microseismic Signal

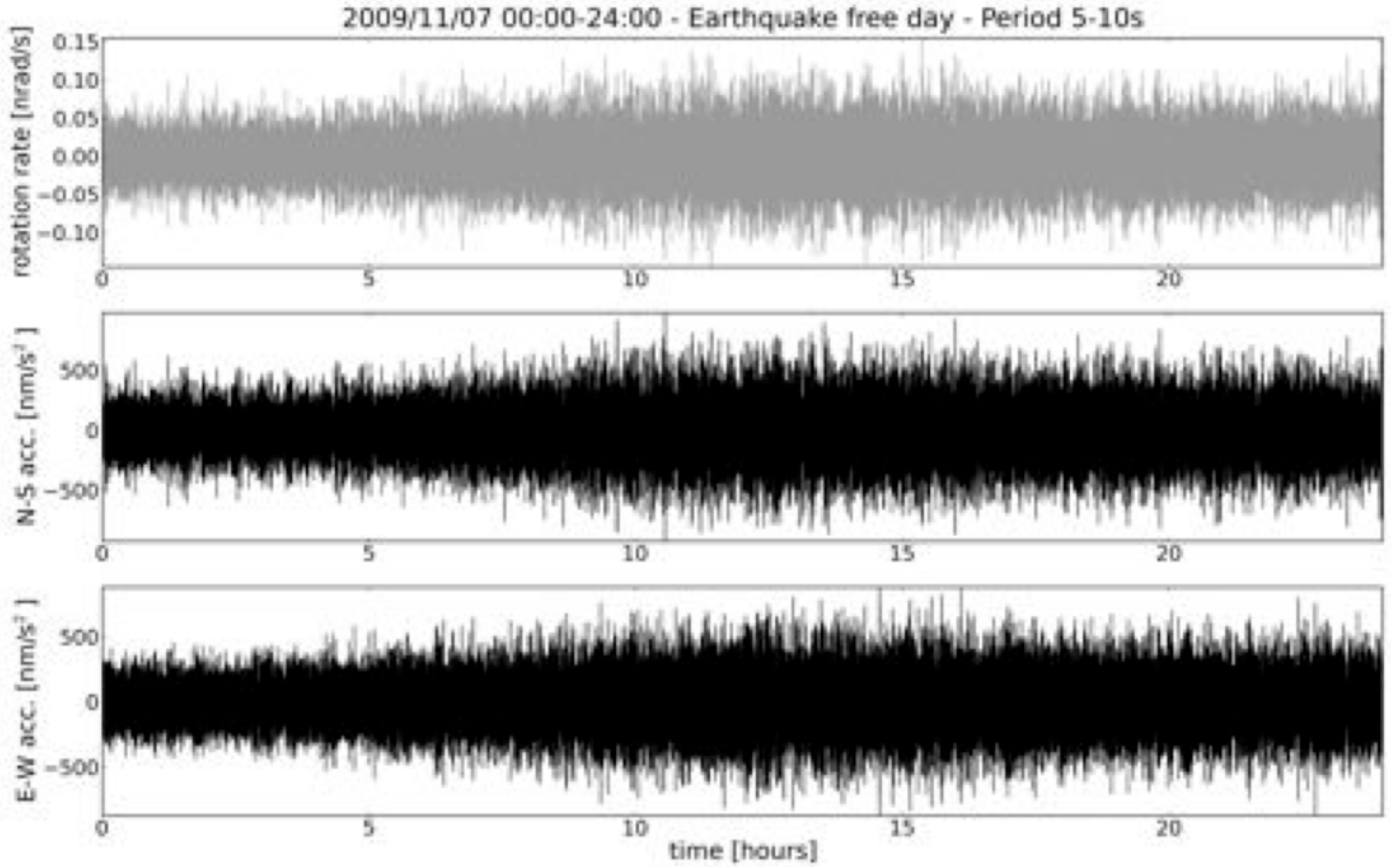

A clear correlation is also apparent in the comparison

There is a surprising high Consistency in this Procedure

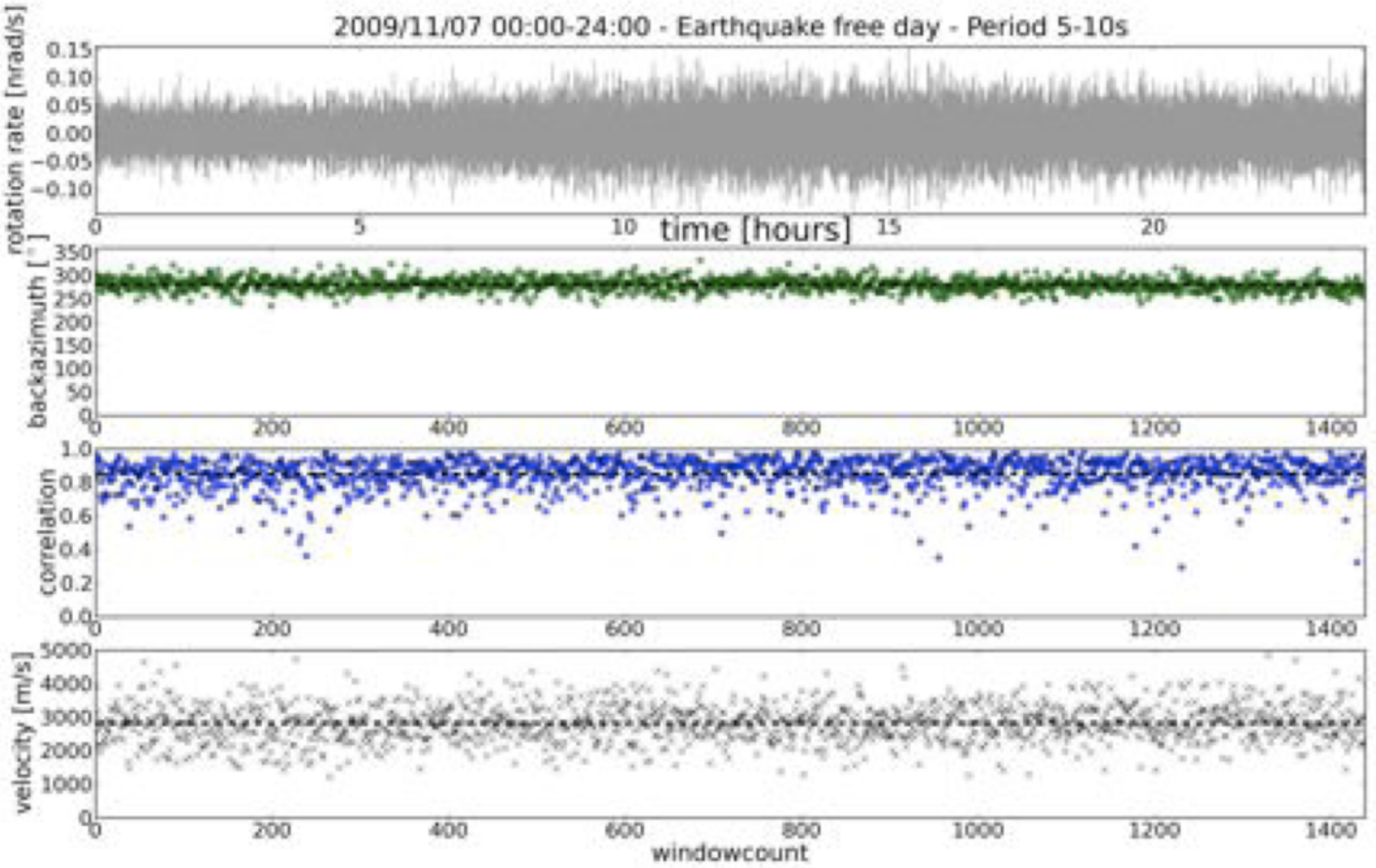

Rotation rate

Back azimuth

Correlation coefficient

Phase velocity

Total length 24 hours, window length 1 minute

In order to get the transversal acceleration, one has to rotate the signal of the two horizontal seismometer components to the correct back-azimuth.

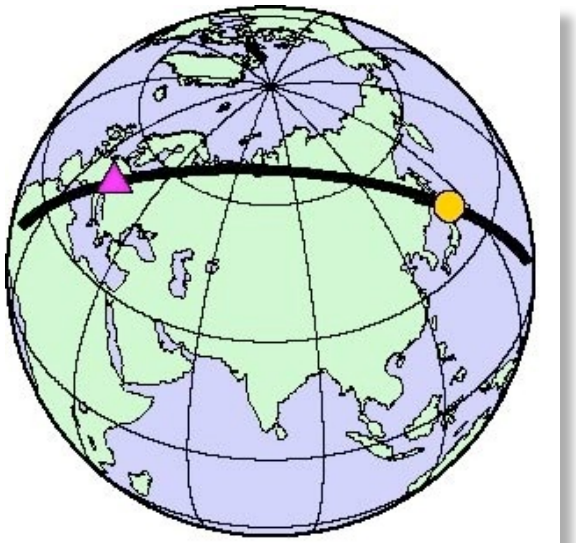

$$\varepsilon = a_x \cos\varphi + a_y \sin\varphi$$

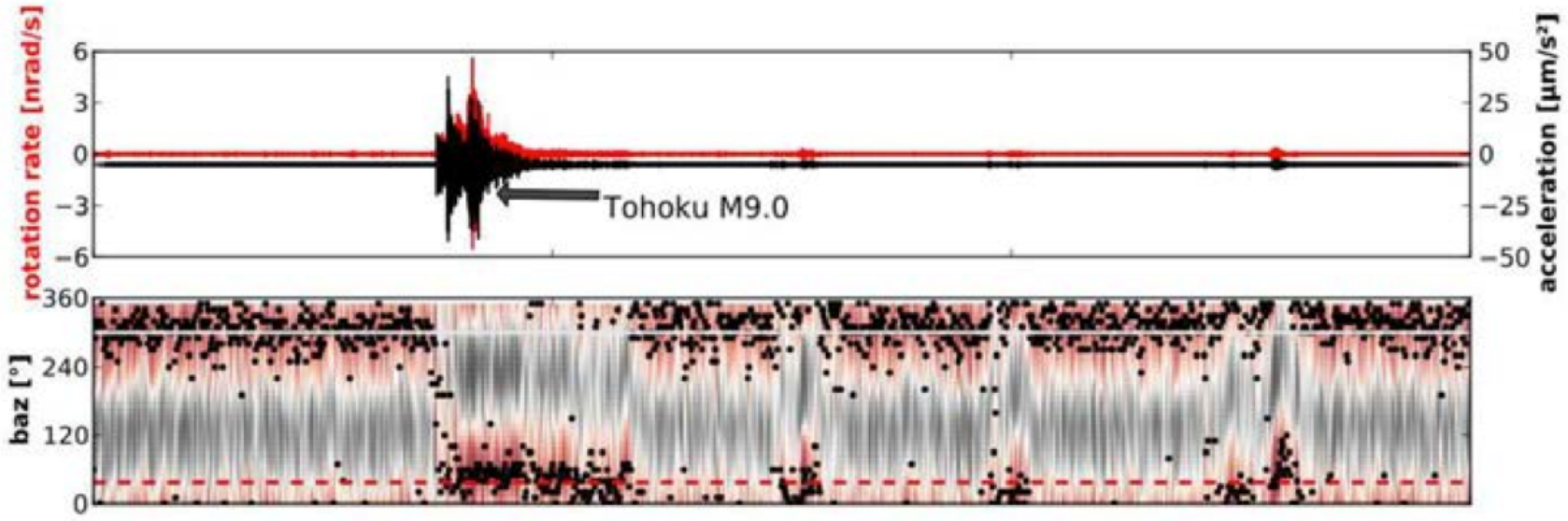

Love Surface Waves cycling around the Earth 4 times (first observation!)

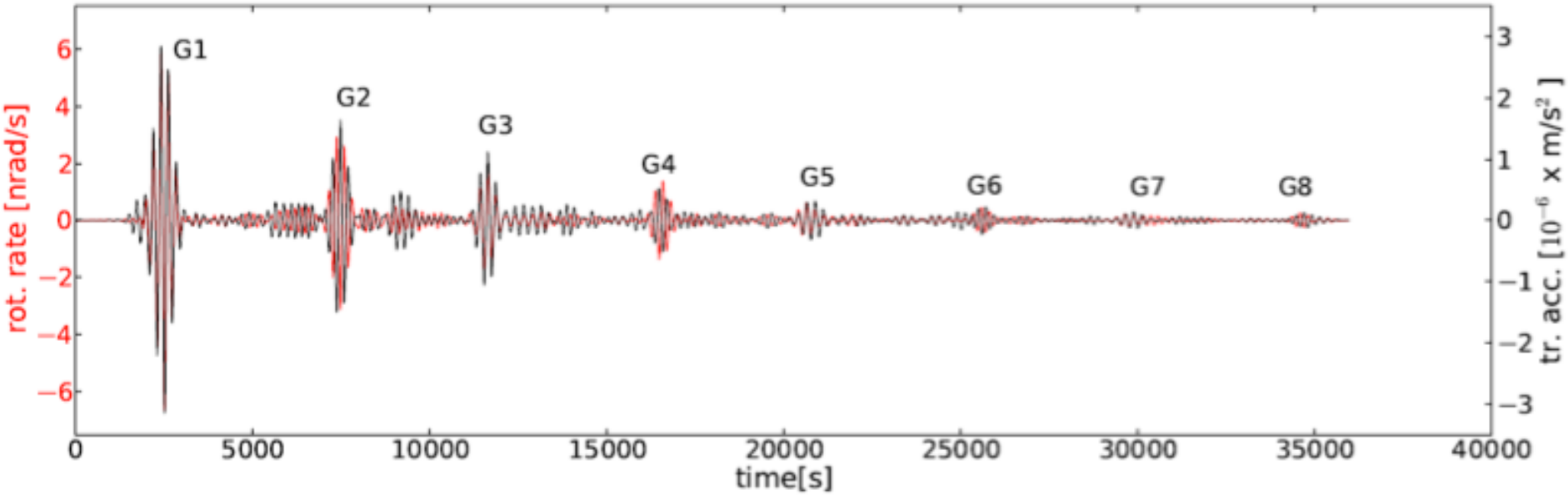

RLG (red) and Seismometer (black)

G1, G3, G5, G7: Signal directly coming from Japan to Wettzell (going west)
G2, G4, G6, G8: Waves going via North America to Wettzell (going east)

Eigenmodes of the Earth

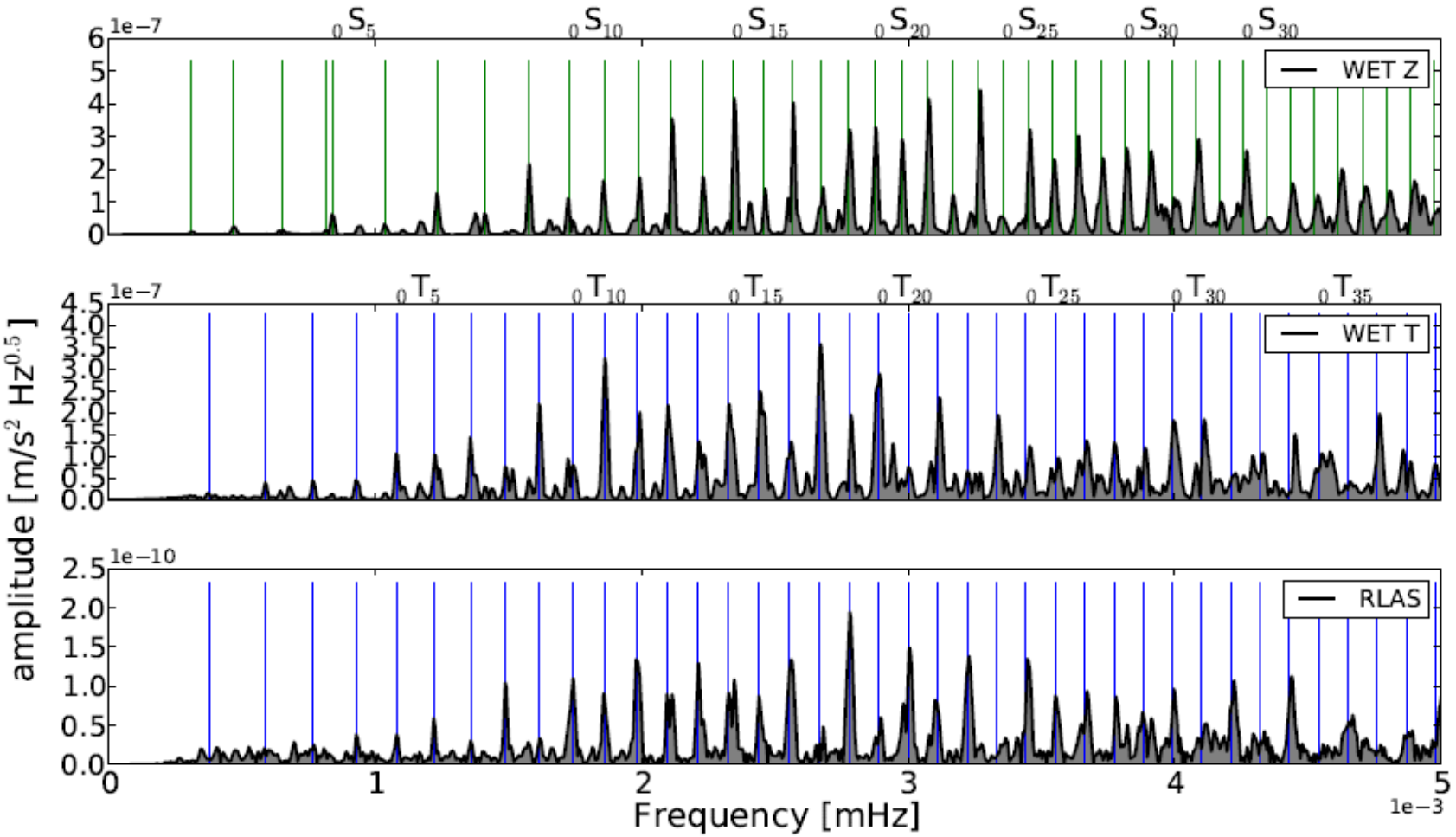

RLG Observation of Eigenmodes (standing Waves) of the entire Earth
RLG (bottom) and Seismometer in Wettzell

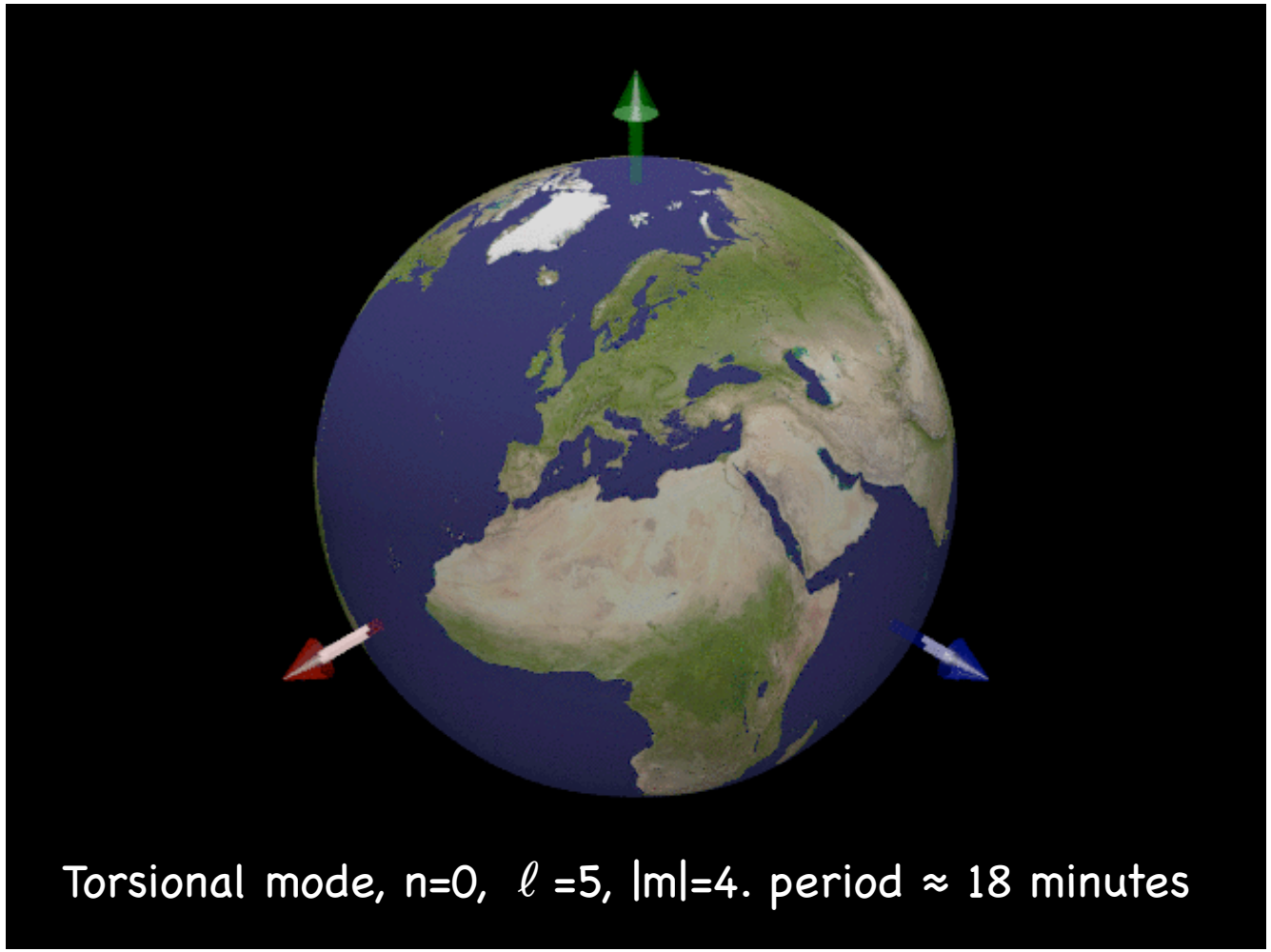

Source: http://icb.u-bourgogne.fr/nano/MANAPI/saviot/terre/index.en.html

Remaining Signature on the Interferogram

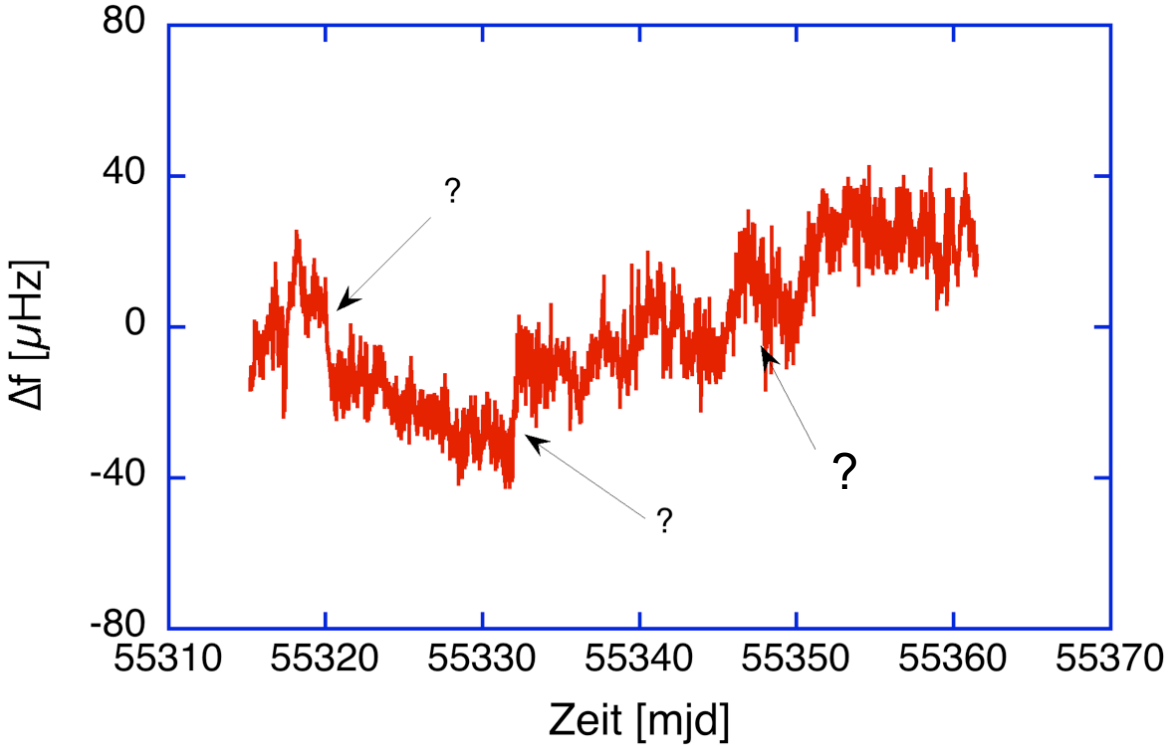

- Backscatter Variations remain to be the most prominent Error Source

cavity stabilization -> backscatter phase constant

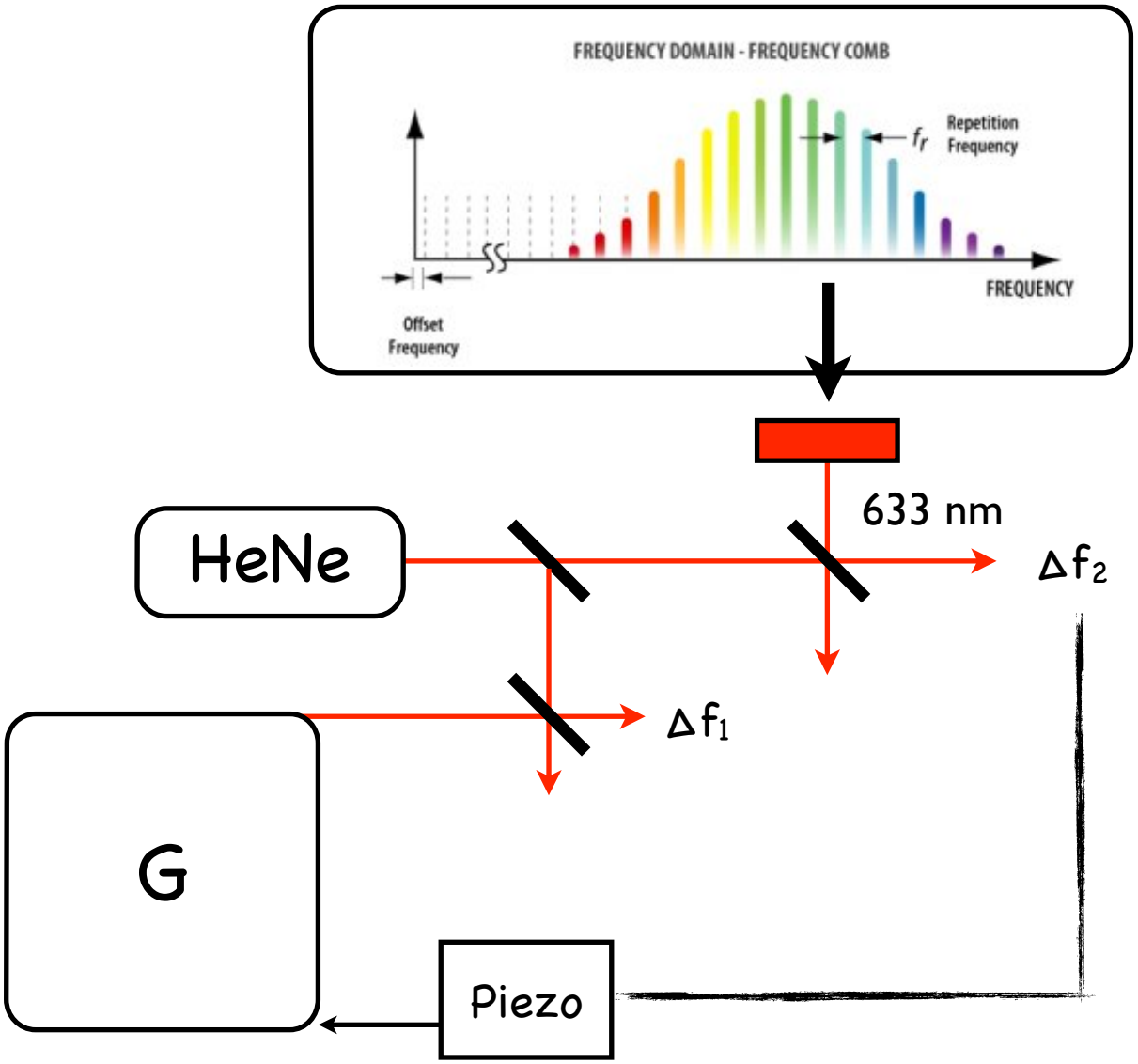

$\Delta f_{opt.} \approx 1\ kHz_{pp}$

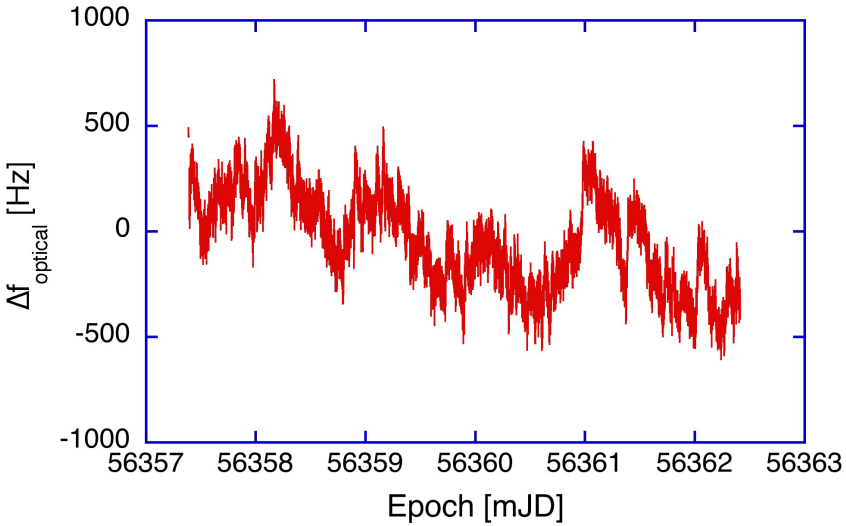

over about 1 week

Raw data in 2012

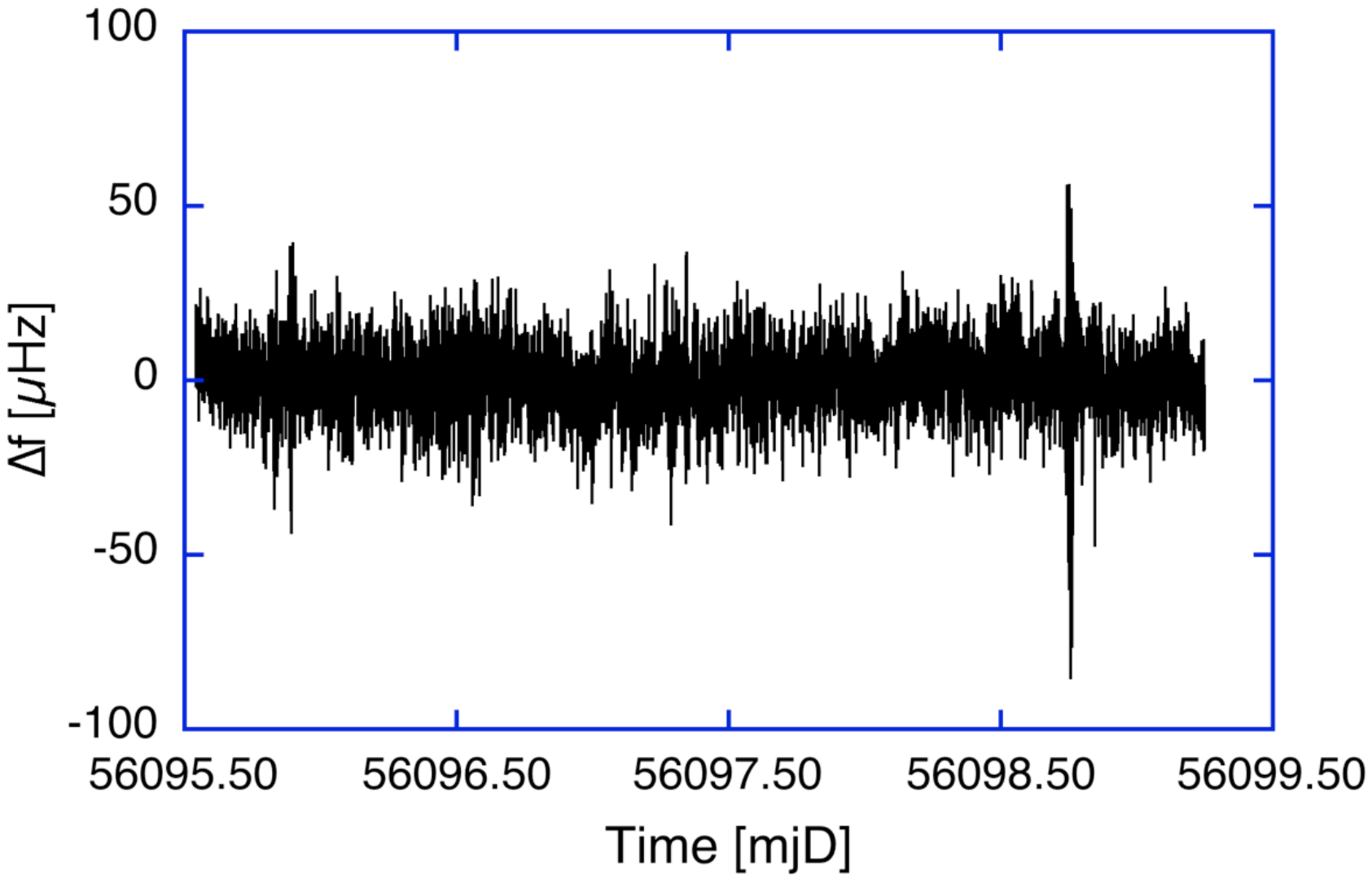

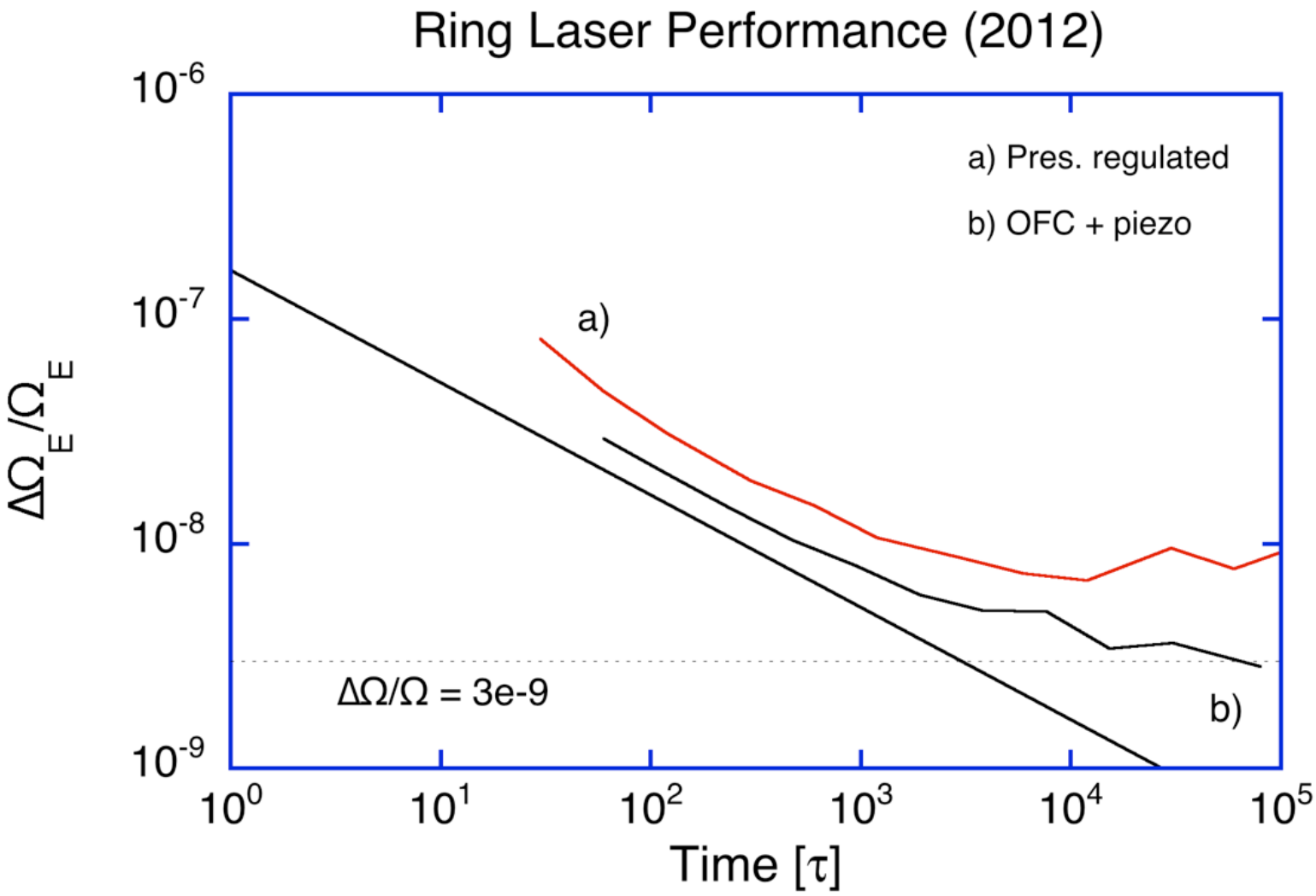

This result is based on perimeter stabilization, backscatter however is depending on the variation of all mirror distances

Backscatter effects:

Backscatter coupling between the clockwise and counterclockwise beams is usually the largest source of systematic error.

$$\Delta f_S \approx \tfrac{1}{2} f_S \; m_1 m_2 \cos\varphi$$

where m_1 and m_2 are the fractional beam modulations, and φ is the phase angle between them.

For given mirror quality, m_1 and m_2 scale approximately as $L^{-2.5}$ for cavity of linear size L.

$\Delta f_S / f_S$ scales approximately as L^{-5} !!!

It is extremely important to maximize the size of the laser, but keep it stable.

Strategy for the correction of backscatter effects:

- Currently under investigation.
- (Obvious first step) Select best available mirrors
- Most promising approach then appears to be a calculated correction based on modulation of the clockwise and counterclockwise beams.

Result for G-0 laser

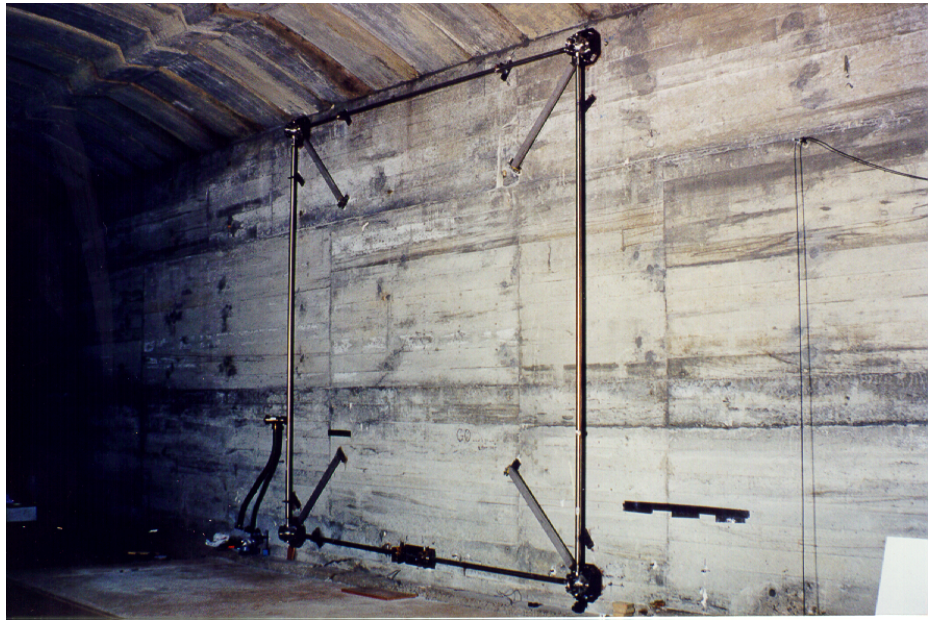

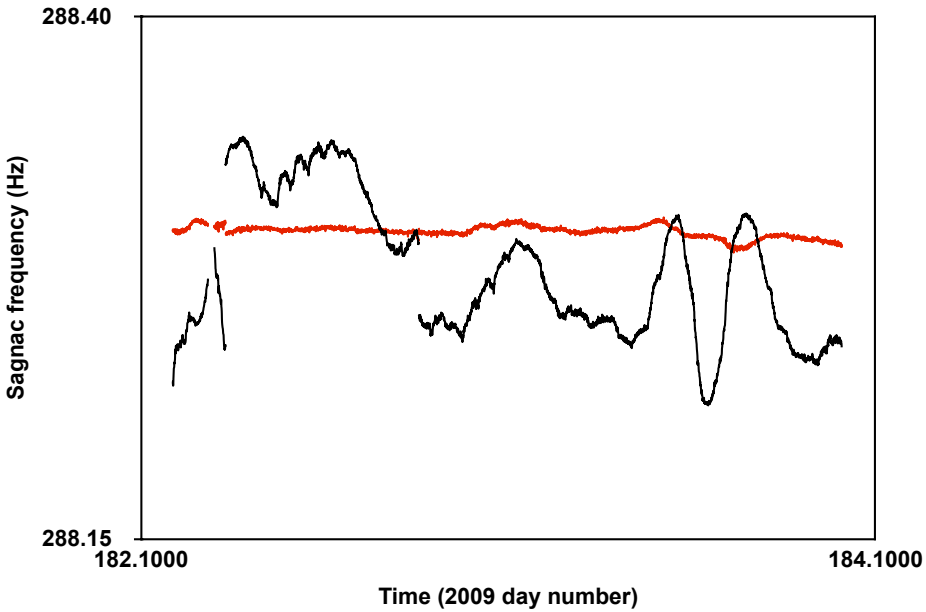

Backscatter Correction

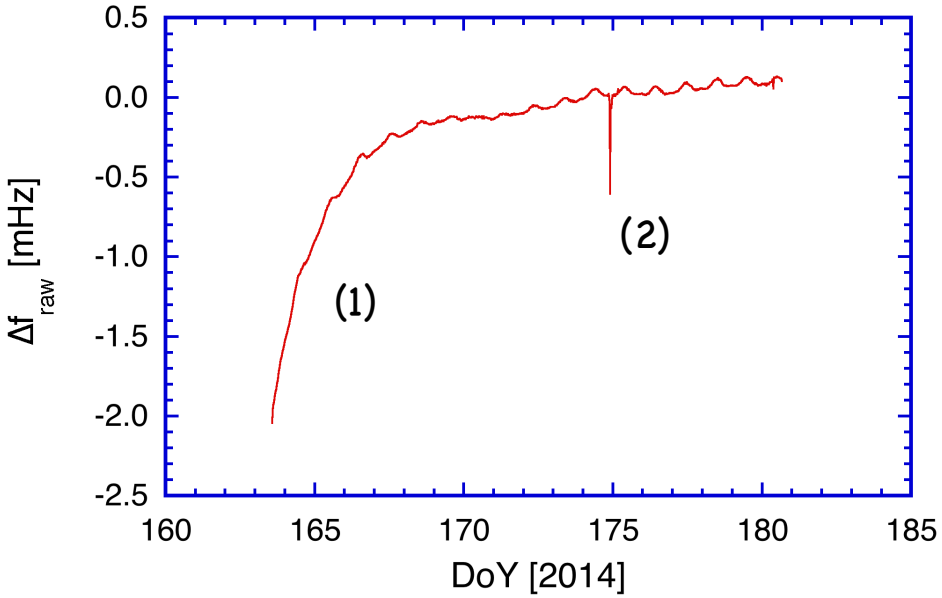

- raw data
- laboratory cooling after detector installation (1)
- mode jump (2)

- corrected data
- pmt and silicon pin diode operation
- pmt showed a significant linear drift

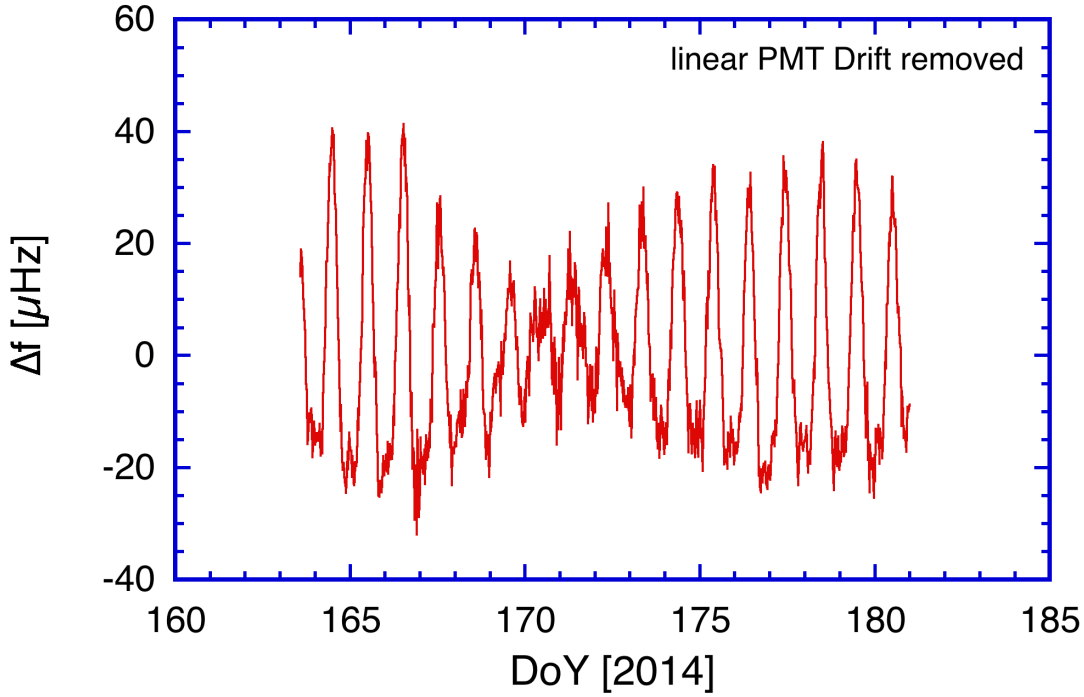

Backscatter Correction

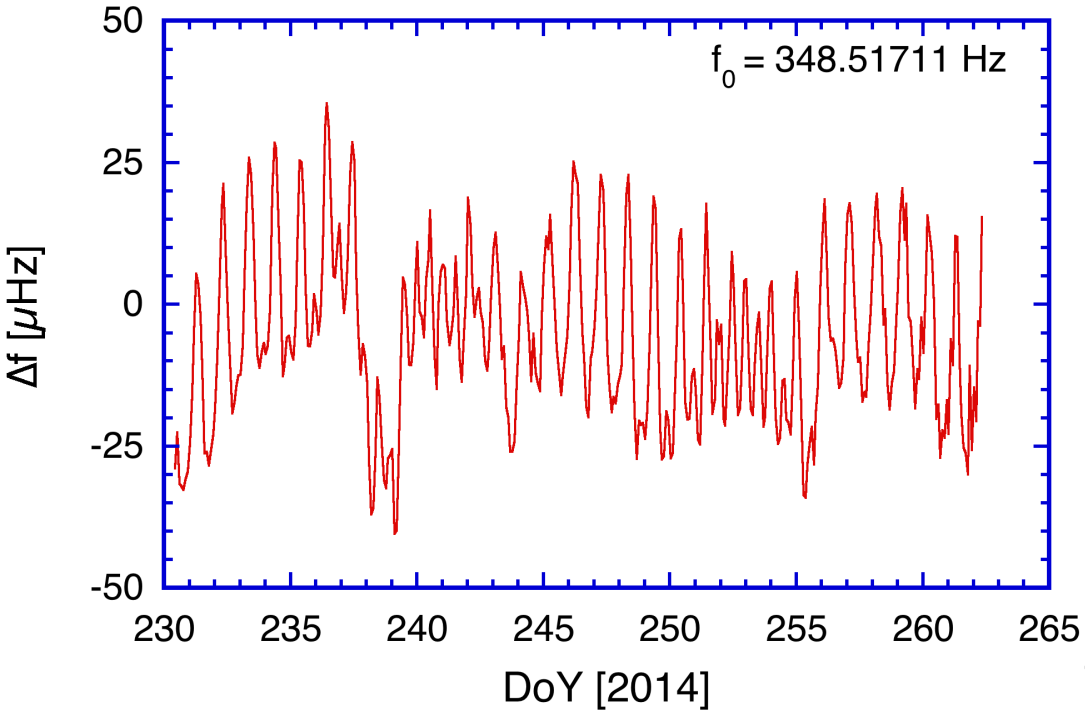

Correction with two solid state detectors and pressure tank open

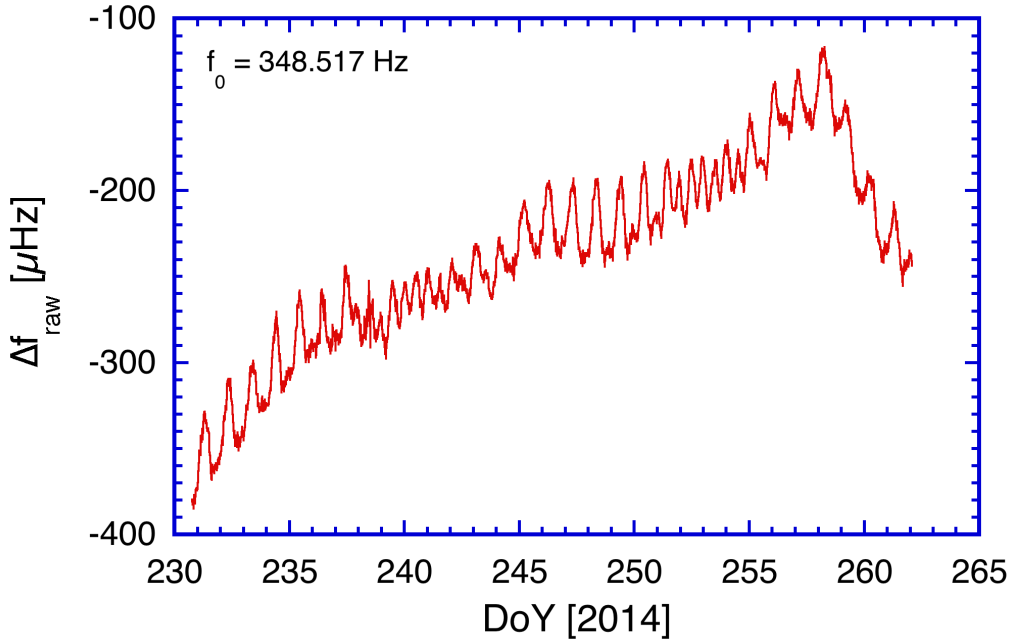

Scalefactor or Detector Systematics?

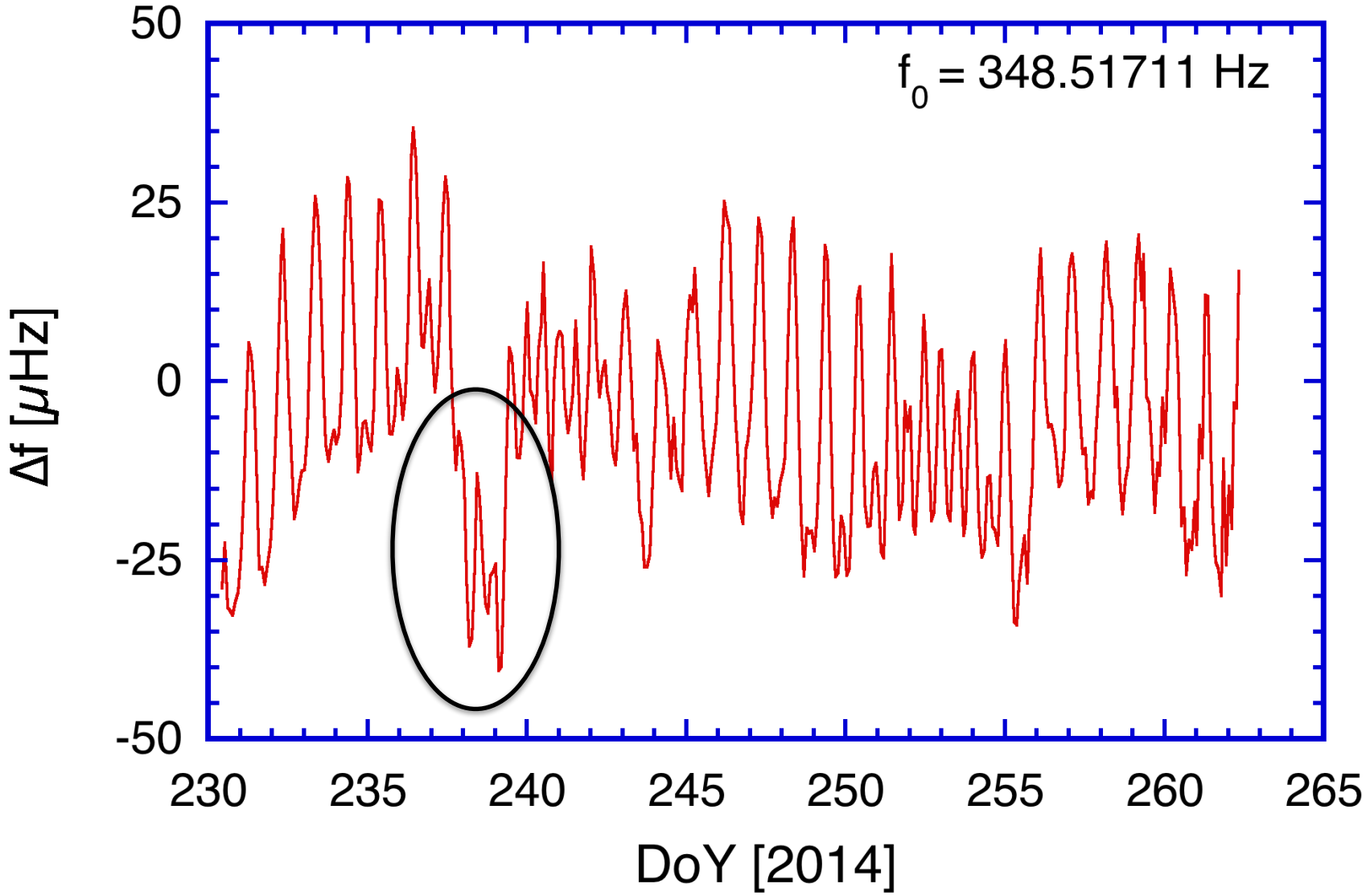

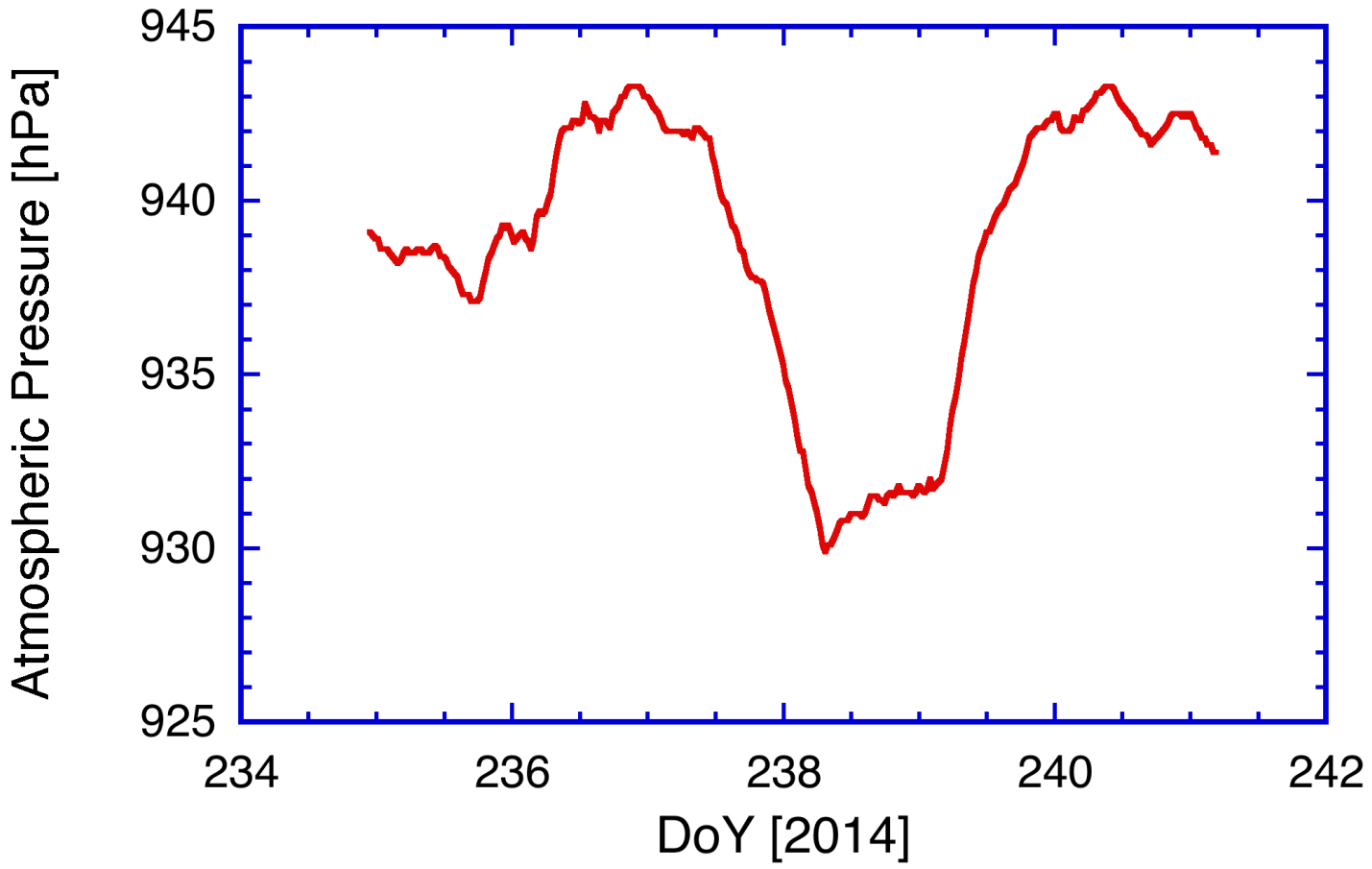
945
940
935
930
925
Atmospheric Pressure [hPa]
234
236
238
240
242
DoY [2014]

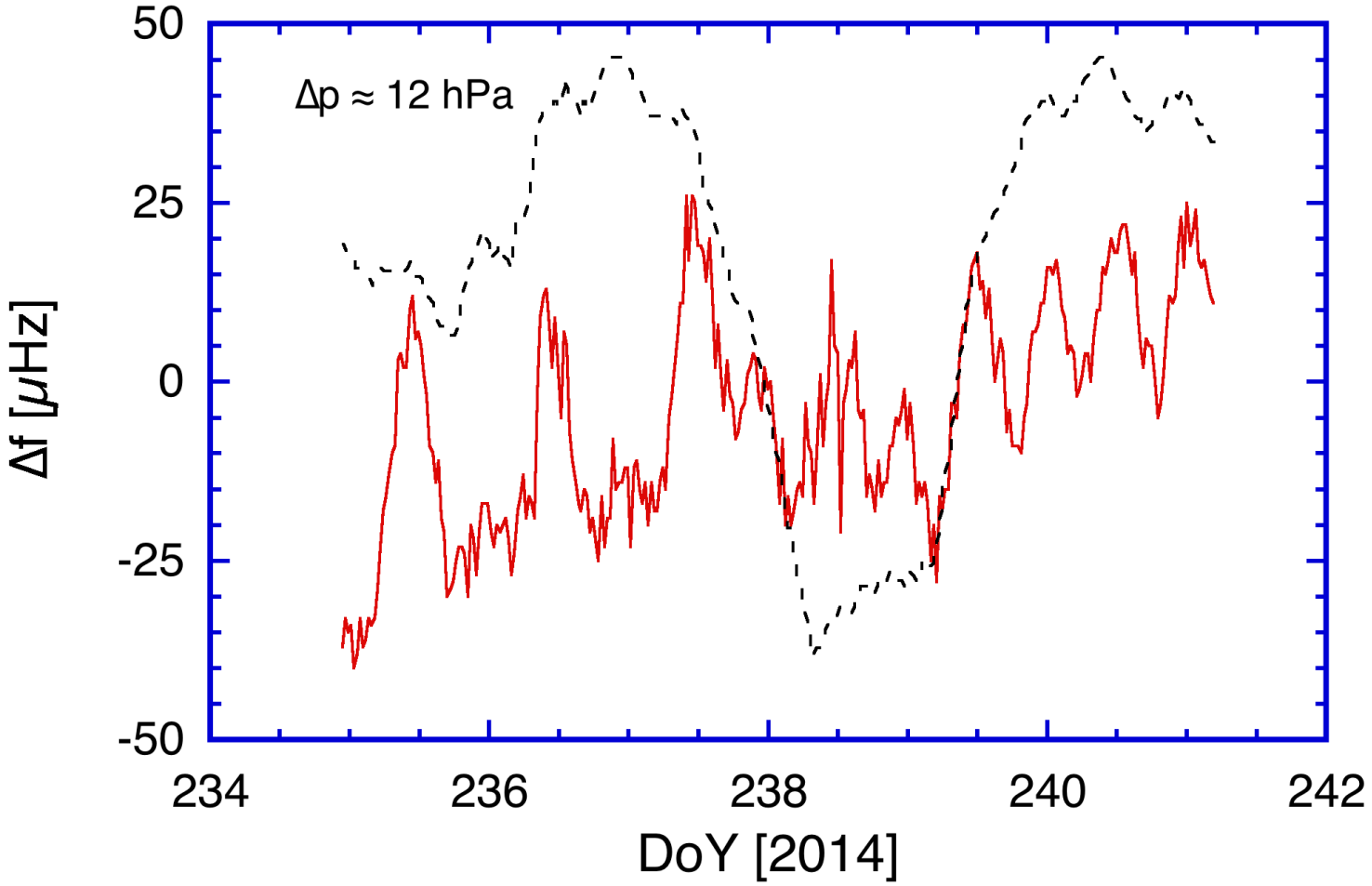
Δp ≈ 12 hPa
50
25
0
-25
-50
Δf [μHz]
234
236
238
240
242
DoY [2014]

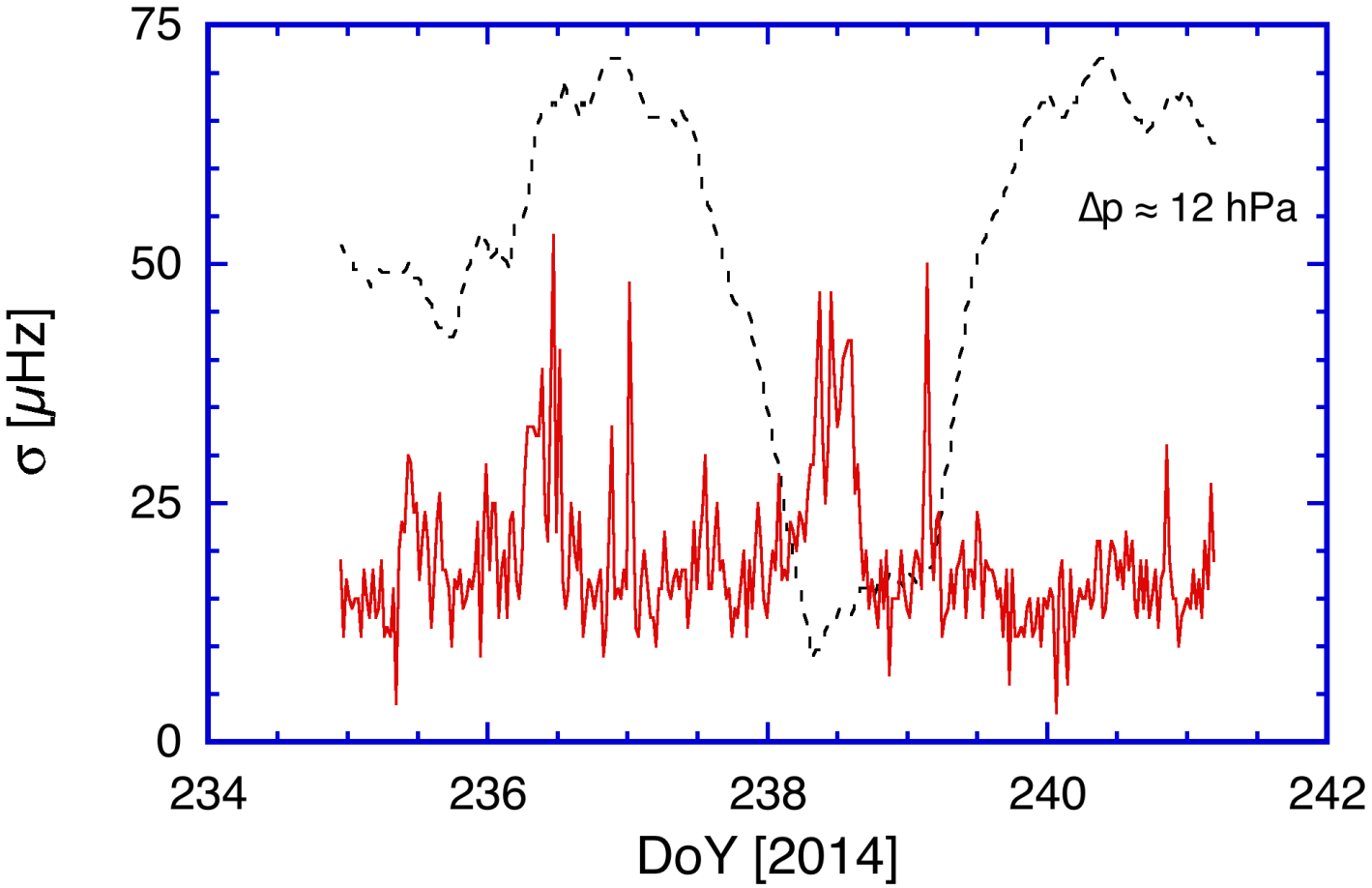
75
50
25
0
σ [μHz]
234
236
238
240
242
DoY [2014]
Δp ≈ 12 hPa

Future Sagnac Interferometer for Fundamental Physics

- 3D- Sensor
- Larger Scale Factor
- Active Stabilization
- Deep Underground Installation

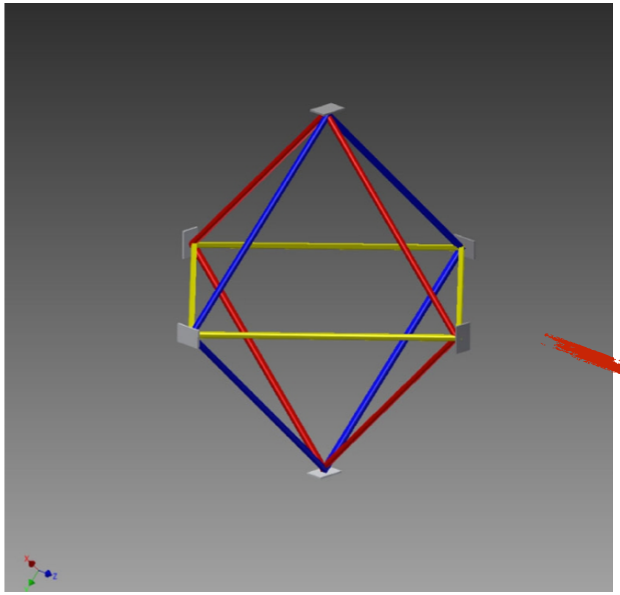

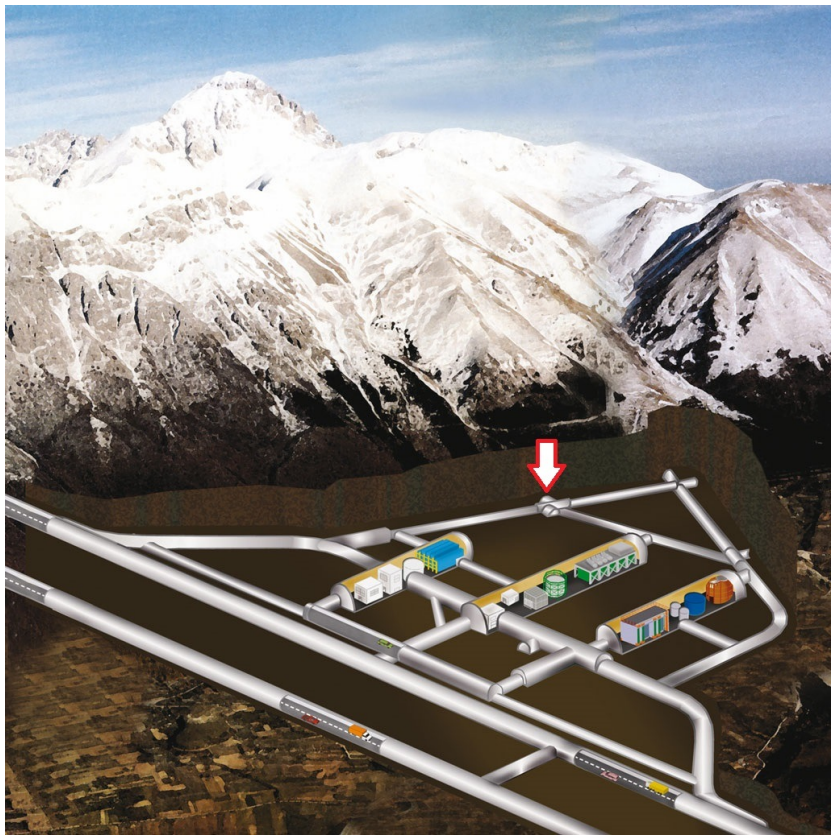

Shared Cavities with control of diagonals...

... however we are after a DC quantity!!!!

We acknowledge contributions from:

University of Canterbury
New Zealand

Geoff Stedman
Jon-Paul Wells
Robert Hurst
Robert Thirkettle

LMU München
Germany

Heiner Igel
Joachim Wassermann
Celine Hadziioannou
Maria Nader

TUM, BKG (Wettzell)
Germany

Alexander Velikoseltsev
Thomas Klügel
Andre Gebauer

INFN, University of Pisa
Italy

Angela Di Virgilio
Nicolo Beverini
Jacopo Belfi
Rosa Santagata

...and many more